Characterization of the FHA domain involved in *Saccharomyces cerevisiae* dNTP regulation

by

Geburah Straker

A thesis
presented to the University of Waterloo
in fulfillment of the
thesis requirement for the degree of
Master of Science
in
Biology

Waterloo, Ontario, Canada, 2018

AUTHOR'S DECLARATION

I hereby declare that I am the sole author of this thesis. This is a true copy of the thesis, including any required final revisions, as accepted by my examiners.

I understand that my thesis may be made electronically available to the public.

Abstract

Over 2000 Forkhead-associated (FHA) domain-containing proteins exhibiting diverse functions, such as kinases, phosphatases, and transcription factors, have been identified to date in both eukaryotic and prokaryotic organisms. Initially characterized as the only known protein-protein interaction motif with phosphothreonine (pThr)-binding specificity, research from the Duncker Lab that characterized the minimal interaction surfaces between the Rad53 FHA1 domain and the Dbf4 H-BRCT domain in the model organism *Saccharomyces cerevisiae* demonstrated the existence and importance of a conserved non-canonical binding surface on Rad53 FHA1 that does not rely on the phosphothreonine-binding patch. Recent analysis by the Duncker Lab of a Rad53 paralog called DNA damage UNinducible (Dun1), a budding yeast cell cycle checkpoint kinase involved in regulating dNTP synthesis, identified another instance of a conserved non-canonical FHA domain lateral surface interaction patch, located on the Dun1 FHA domain, similar to that of Rad53 FHA1. Continued examination of the Dun1 FHA domain lateral surface interaction patch and pThr-binding site suggested the existence of a differential requirement for the non-canonical FHA domain lateral surface interaction patch and the canonical pThr-binding site during interactions between Dun1 and some of its ligands.

The research presented in this thesis aimed to study the prevalence of protein-protein interactions in *S. cerevisiae* that operate using this novel non-canonical lateral surface interaction patch of FHA domains as well as their functional significance in cell growth and survival mechanisms in response to genotoxic stress, using the Dun1 FHA domain as an example. In order to investigate the existence and importance of Dun1 non-canonical FHA domain-based protein-protein interactions, bioinformatics analysis was used to identify candidate conserved residues on the FHA domain lateral surface interaction patch, site-directed mutagenesis was used to alter select amino acids and yeast two-hybrid assays were used to compare disruptions and/or the abrogation of protein-protein interactions between wild type and

mutant Dun1 FHA domains with ligands involved in dNTP regulation. Analysis of the interaction between the FHA domain of Dun1 and proteins involved in the dNTP regulation pathway illustrated a differential requirement of the FHA domain lateral surface interaction patch and the pThr-binding site as well as a contribution of the kinase domain for the establishment of at least two interactions. Highly conserved residues of the Dun1 FHA domain lateral surface interaction patch contributed to FHA domain-based protein-protein interactions and slight but reproducible genotoxic sensitivity was observed for Dun1 FHA domain mutants. The interaction between Dun1 and Damage-regulated Import Facilitator (Dif1) suggested a contribution of the kinase activity of the Dun1 kinase domain to the establishment of a maximal interaction. In order to observe any interaction between Dun1 and Suppressor of *mec1* lethality (Sml1), both the FHA and kinase domains needed to be present. Mutation of the conserved arginine 60 (R60A) residue of the canonical pThr-binding site completely disrupted the interaction between Dun1 and Dif1 whereas it only weakened the interaction between Dun1 and Sml1. Single mutations of the conserved asparagine 121 (N121A) and leucine 134 (L134A) of the non-canonical FHA domain lateral surface interaction patch did not affect the interaction between Dun1 and Dif1, but mutation of the conserved lysine 136 (K136A) within the context of just the Dun1 FHA domain increased the strength of the interaction between Dun1 and Dif1. The N121A single mutation had no affect on the interaction between Dun1 and Sml1 while both the L134A and K136A single mutations decreased the strength of the interaction between Dun1 and Sml1. The R60A, N121A, L134A, and K136A single mutants showed decreased growth in response to genotoxic stress, illustrating the importance of Dun1 interactions that utilize conserved residues of the non-canonical FHA domain lateral surface interaction patch and the canonical pThr-binding site to genotoxic stress responses in budding yeast.

Acknowledgements

I would like to thank my supervisor, Dr. Bernard Duncker, for giving me the opportunity to work in his lab. As a supervisor, his expectations give his students the ability to learn how to work efficiently and successfully while also having fun with their research. I would like to thank my committee members Dr. Brendan McConkey and Dr. Christine Dupont. Thank you for all of your guidance and suggestions. You have both been extremely easy to work with, especially for scheduling committee meetings, and I greatly appreciate your interest in my work. I would also like to thank all of the faculty and staff of the Department of Biology who have in any way contributed to my success as a student here at the University of Waterloo.

Thank you to all of the Duncker lab members for being both accommodating and helpful. I would not have learned as much as I have without all of you. Thank you for keeping me 'on my toes' and for making every day interesting. I wish everyone the best of luck in their future endeavors. Special thanks to Darryl Jones, Damir Mingaliev, Aaron Robertson, and Alison Guitor who have all made contributions to the topic of FHA domain research in the Duncker Lab.

Above all, I'd like to thank my parents for all of the support and guidance that has led me to where I am today and where I will be tomorrow.

Table of Contents

List of Figures

List of Tables

List of Abbreviations

Cdc: Cell division cycle

CDK: Cyclin dependent kinase

DDK: Dbf4 dependent kinase

DNA: Deoxyribonucleic acid

dNTP: Deoxyribonucleoside triphosphate

DTT: Dithiothreitol

EDTA: Ethylenediaminetetraacetic acid

FHA: Forkhead-associated

FL: Full-length

GAL/RAF: Galactose/Raffinose

HA: Hemagglutinin

H-BRCT: Helix-BRCA 1 Carboxy-terminal

HU: Hydroxyurea

Kb: kilobases

kDa: kilodalton

MMS: Methyl methanesulfonate

MYC: Myelocytamatosis

ONPG: 2-Nitrophenyl-β-D-galactopyranoside

PCR: Polymerase chain reaction

PMSF: Phenylmethylsulphonyl fluoride

RNR: Ribonucleotide reductase

SC: Synthetic complete

SDS: Sodium dodecyl sulfate

WCE: Whole cell extract

WT: Wild-type

YPD: Yeast extract, peptone, dextrose

Chapter 1

Introduction and Research Objectives

1.1 *Saccharomyces cerevisiae* and the Cell Cycle

Model organisms are and have consistently been fundamental tools for studying biological processes, as proxies for studying the same or similar processes in higher eukaryotes. The most effective model organisms are those that are easy to grow, control, manipulate and maintain. One model organism prominent for its use in studying the molecular biology of the cell cycle and cell cycle checkpoints, largely contributing to the breadth of knowledge acquired under the 'umbrella' of cancer research, are yeasts.

1.1.1 Budding Yeast Model Organism

The taxonomic definition of yeast, of which there are thousands of species, is that yeasts are single-celled eukaryotic micro-organisms of the fungus kingdom that can grow and function with or without oxygen (reviewed in Mortimer, 2000). These facultative anaerobes utilize fermentation to break down sugars into carbon dioxide and ethanol (reviewed in Mortimer, 2000). In general, yeasts are easy to grow and maintain, with a typical doubling time of approximately 90 minutes under an optimal laboratory-constructed environment of sugar and nitrogen-based media, and they are easy to manipulate physically and genetically (reviewed in Duina et al., 2014, Gershon and Gershon, 2000, Herskowitz, 1988, and Mortimer and Johnston, 1986). *Saccharomyces cerevisiae*, budding yeast, is one of two main species of yeast used extensively for cell cycle research, and was used throughout the research presented in this thesis (reviewed in Gershon and Gershon, 2000). The 'budding yeast' common name describes a distinguishing characteristic of this yeast where cell proliferation is achieved through an asymmetrical

division of a 'mother cell' generating a 'bud' that pinches off from the 'mother cell' (reviewed in Duina et al., 2014).

Budding yeast exhibit many of the features that make a model organism useful. In addition to being unicellular with a relatively short generation time, the relatively small genome of budding yeast has been completely sequenced and extensively mapped at just over 12, 000 kilo bases (Kb) organized as 16 chromosomes in the haploid genome (Goffeau et al., 1996; reviewed in Gershon and Gershon, 2000). Budding yeast characteristics have also been useful in the design of a wide variety of molecular biology tools for studying genetics, cell biology and the cell cycle (reviewed in Gershon and Gershon, 2000). The intricate control over cell cycle progression and the ability to switch between mitosis and meiosis have allowed for the development of tools such as the ability to add chemicals or mating factors to a cell culture to stall cell cycle progression in order to synchronize progression for a culture of cells as well as generating and maintaining cells in a haploid state to be studied (reviewed in Gershon and Gershon, 2000). The mechanisms of genetic recombination in budding yeast have been exploited to develop a large collection of genomic knockout yeast strains used by many yeast researchers (reviewed in Gershon and Gershon, 2000). Additionally, the budding yeast genome contains a large number of orthologs to human disease-causing genes and genes involved in similar, if not conserved, biological pathways (reviewed in Gershon and Gershon, 2000).

Budding yeast can exist as any of three possible cell types: (1) Mating type a (*MATa*) haploid cells, (2) Mating type α (*MATα*) haploid cells, or (3) Mating type a/α (*MATa/α*) diploid cells (reviewed in Herskowitz, 1988 and Duina et al., 2014). Located on chromosome III, the *MAT* locus will have one of the two nonhomologous *MAT* alleles, either *MATa* or *MATα*, containing the genetic information that determines the mating type (reviewed in Duina et al., 2014). The two haploid cells each secrete mating type-specific peptides as mating factors, mating pheromones, which allow the *MATa* and *MATα* haploid cells to mate with each other to form the *MATa/α* diploid (reviewed in Herskowitz, 1988 and Duina et al., 2014). *MATa* and *MATα* haploid cells undergo mitosis for cellular proliferation or fuse to form a *MATa/α*

diploid cell which also undergo mitosis for cellular proliferation or meiosis for gamete production during times of nutrient starvation (reviewed in Herskowitz, 1988 and Duina et al., 2014).

Both heterothallic and homothallic yeast strains were found on rotting figs during the late 1800s - early 1900s and were used by yeast geneticists, Ojvind Winge and Carl Lindergren, to pioneer the use of yeast for research (Mortimer and Johnston, 1986; reviewed in Mortimer, 2000 and Duina et al., 2014). Heterothallism refers to the inability of a haploid yeast cell to switch mating types due to a lack of functional HO endonuclease, encoded by the *HO* ("Homothallism") gene, which is responsible for the transposition of an *HMLα* or *HMRa* genetic cassette from a location where it is silenced to the location of the *MAT* locus where it will be expressed (Mortimer and Johnston, 1986; reviewed in Herskowitz, 1988, Mortimer, 2000 and Duina et al., 2014). Homothallic cells, for which the *HO* gene and endonuclease were named, are able to switch mating types because they do have functional HO endonuclease (reviewed in Herskowitz, 1988 and Duina et al., 2014). The *HMLα* and *HMRa* genetic cassettes contain the same genetic information expressed at the *MATα* and *MATa* loci respectively (reviewed in Herskowitz, 1988). Most yeast strains used for research, including the research presented in this thesis, were derived from a heterothallic yeast strain isolated by a pioneer of yeast genetics, Emil Mrak in 1891 (reviewed in Mortimer and Johnston, 1986 and Duina et al., 2014).

1.1.2 The Cell Cycle

The cell cycle refers to the progression of a cell through stages of growth, replication, and division. Typical eukaryotic cells exhibit a consistent pattern of progression through the cell cycle; however the precise steps that occur in each stage may differ among organisms (reviewed in Herskowitz, 1988). That consistent pattern of cell cycle progression entails a Gap 1 (G_1), Synthesis (S), Gap 2 (G_2), and mitosis phase (Figure 1.1). During G_1 phase, cells exhibit continual growth to prepare for ensuing deoxyribonucleic acid (DNA) replication during the S phase (reviewed in Herskowitz, 1988). Additionally during G_1, eukaryotic cells regulate the association of multiple DNA replication initiation

factors at sites of DNA replication initiation referred to as origins of replication in a process called origin licensing (Shirahige et al., 1998; Duncker et al., 2002; reviewed in Matthews et al., 2012). The G_0 phase represents a quiescent stage of the cell cycle where cells in G_1 phase can rest if conditions are not optimal for commitment to DNA replication and cellular division such as poor nutrient availability, present compatible mating pheromones, or inadequate cell size (reviewed in Herskowitz, 1988; Figure 1.1). The START point of the cell cycle, highly regulated and influenced by nutrient availability, presence of compatible mating pheromones, and cell size, represents the point during late G_1 phase when cells commit to entrance into S phase (reviewed in Hiroshima et al., 2013 and Herskowitz, 1988; Figure 1.1). The S phase represents the stage of the cell cycle during which DNA is replicated via semi-conservative replication at 'licensed' origins of replication which have accumulated all of the required replication initiation factors (reviewed in Hiroshima et al., 2013). The G_2 phase is a secondary period of growth for most eukaryotic cells during which they truly prepare to separate all duplicated cellular components in addition to dividing replicated DNA (reviewed in Herskowitz, 1988). The M phase primarily features the physical segregation of replicated genetic material over the duration of four stages: Prophase, Metaphase, Anaphase, and Telophase which can be mostly identified by the physical appearance of the DNA and cellular components (reviewed in Herskowitz, 1988). Typically, the actual physical separation of the resulting daughter cell(s) and their cytoplasm occurs after the completion of mitosis, and is referred to as Cytokinesis (reviewed in Herskowitz, 1988). In eukaryotic cells, mitosis features the segregation of genetic content to opposite poles of the parent cell via the spindle microtubules (reviewed in Balasubramanian et al., 2004). The formation of a contractile actomyosin ring at the 'division plane' between the two poles orchestrates the cytoplasmic separation seen during cytokinesis, and continual contraction of the actin ring pinches the cytoplasm between the two poles until two distinct daughter cells are formed (reviewed in Balasubramanian et al., 2004).

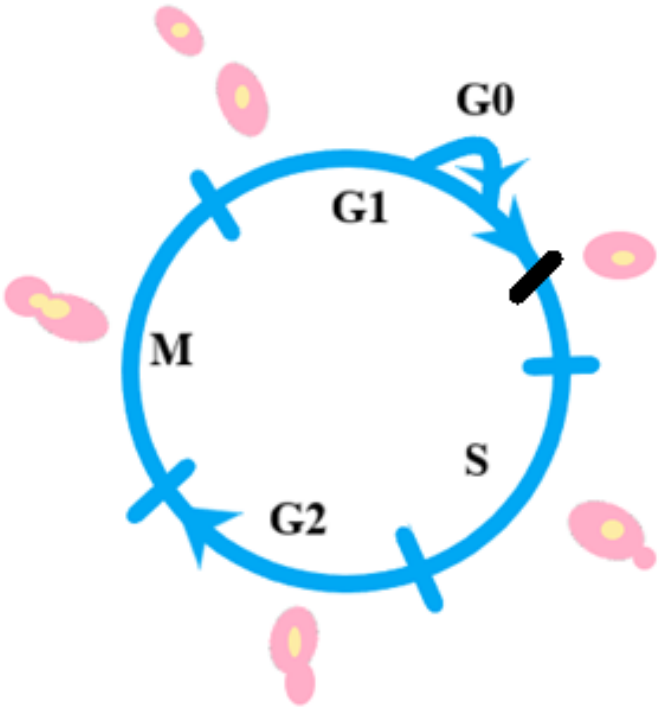

*The budding yeast cell cycle does not feature an actual G2 phase as shown for the typical eukaryotic cell cycle.

Figure 1.1: Eukaryotic Cell Cycle and *Saccharomyces cerevisiae*

Depiction of the mitotic cell cycle illustrating the order and approximate duration of each phase of the cell cycle: Gap1 (G_1), Synthesis (S), Gap 2 (G_2), and Mitosis (M) as well as bud formation from the mother cell generating the smaller daughter cell. Resting stage (G_0) refers to a quiescent stage during which the cell cycle is arrested. Pink and yellow circles represent yeast cell(s) and nuclei, respectively. The solid black line indicates the START point of S phase entry commitment (adapted from Herskowitz, 1988).

In contrast to the general eukaryotic mitotic cell cycle, the budding yeast cell cycle does not feature an actual G_2 phase due to the formation of the mitotic spindle during S phase (Gershon and Gershon, 2000; Figure 1.2). Additionally, since bud formation (shown in Figure 1.1) results in a daughter cell that is smaller than the mother cell, the duration of the G_1 phase is extended to compensate for the additional time required for the daughter cell to grow to its 'adult' size in preparation for its own entrance into cell division and in order to get past the START checkpoint (Gershon and Gershon, 2000). Unlike animal cells, budding yeast cells possess a cell wall and do not exhibit nuclear envelope breakdown

(reviewed in Balasubramanian et al., 2004). As a result, budding yeast cells feature the formation of spindle pole bodies within the nuclear envelope and a septum of cell wall material at the 'division plane' during cytokinesis following the formation of the actomyosin contractile ring (reviewed in Balasubramanian et al., 2004). The spindle pole bodies influence the segregation of replicated genetic material to opposite poles of the nucleus generating two 'daughter nuclei' (reviewed in Balasubramanian et al., 2004). The passage of one of the two 'daughter nuclei' through the 'bud neck' contributes to mitotic exit and cytokinesis in budding yeast (reviewed in Balasubramanian et al., 2004).

The natural progression of the cell cycle is highly regulated by cyclin-dependent protein kinases (CDKs) and their associated cyclin subunits (Nasmyth, 1996; Morgan, 1997). The levels of cyclins tend to oscillate in a manner that mostly matches cell cycle progression and, as a result of their required association with CDKs for kinase activation and signal transduction, contribute to various cell stage-specific processes that influence cell cycle progression (Nasmyth, 1996; Koivomagi et al., 2011; reviewed in Hiroshima et al., 2013). There are five major CDKs in budding yeast: Cdc28, Pho85, Kin28, Srb10, and Ctk1, but only Cdc28 influences proliferation via its control of the cell cycle (Morgan, 1997; reviewed in Hiroshima et al., 2013). Activities associated with G_1 phase are largely controlled by the associations of Cdc28 with the Cln1, Cln2, and Cln3 cyclins (Figure 1.2, Cln3 not shown; Nasmyth, 1996; reviewed in Morgan, 1997 and Koivomagi et al., 2011). S phase is mostly coordinated by Cdc28 associated with the Clb5 and Clb6 cyclins while mitosis is governed primarily by Cdc28 associated with Clb1, Clb2, Clb3, and Clb4 (Figure 1.2; Nasmyth, 1996; reviewed in Morgan, 1997 and Koivomagi et al., 2011). The associations of Cdc28 with specific cyclins as well as the order in which those associations occur generate activities that are mostly phase-specific, however, there is extensive overlap between the timings of cyclin-Cdc28 couplings and the duration of their functions across the cell cycle phases which contributes to the pattern of cell cycle progression in budding yeast (Nasmyth, 1996; reviewed in Morgan, 1997 and Koivomagi et al., 2011).

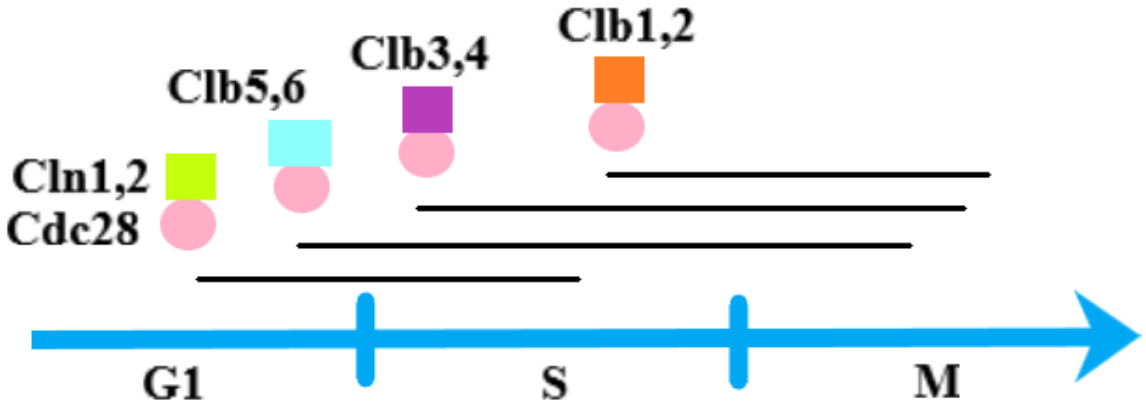

Figure 1.2: Cyclin-CDK Complexes and *S. cerevisiae* Cell Cycle Phase Progression

S. cerevisiae cell cycle and phase progression illustrating the approximate time of initiation and duration of function of the involved cyclin-CDK complexes. Solid black lines indicate duration; initiation to completion is represented from left to right, of cyclin-CDK activity. Pink circles represent the Cdc28 CDK and the squares represent associated cyclins (adapted from Morgan, 1997).

1.1.3 Cell Cycle Checkpoints

Cell cycle checkpoints ensure correct cell cycle progression, cellular growth, duplication of the cellular components, and serve as arrest points of the cell cycle in order to initiate the appropriate repair pathways in response to stress and/or damage (reviewed in Rhind and Russell, 1998). They regulate all of the major transition points of the cell cycle as well as several meiotic transitions, contribute to transcriptional regulation and recovery from cell cycle arrest, ensure proper spindle assembly, DNA replication and damage repair, and, specific to budding yeast, ensure proper bud formation (reviewed in Rhind and Russell, 1998, Longhese et al., 1997, and Barnum and O'Connell, 2014).

In eukaryotes, checkpoints monitoring cell size can occur during the G_1 and G_2 phases, DNA damage checkpoints can occur throughout interphase, and the mitotic spindle checkpoint occurs during metaphase preceding the metaphase-to-anaphase transition to ensure that sister chromatids are attached to the spindle microtubules via the kinetochore and that there is adequate tension in those attachments

(reviewed in Barnum and O'Connell, 2014). The DNA damage response (DDR), triggered by DNA damage, is fundamental to genome stability (reviewed in Longhese et al., 1997). Errors in cell cycle progression and DNA replication, especially errors that are not successfully repaired, often lead to genomic instability and compounding mutations that can manifest in the form of various complex diseases such as cancer (reviewed in Longhese et al., 1997).

In budding yeast, there are four main DNA damage checkpoints that typically deal with DNA damage repair and recovery: (1) the G_1/S checkpoint, (2) the intra-S phase checkpoint, (3) the S/M checkpoint, and (4) the metaphase or G_2/M checkpoint (Siede et al., 1993, 1994; Paulovich and Hartwell, 1995; Weinert and Hartwell, 1988; reviewed in Longhese et al., 1997 and Barnum and O'Connell, 2014). The intra-S phase checkpoint specifically focuses on the stabilization of the complex of DNA polymerase and associated replication factors when replication forks have been stalled due to replication stress or damage and is controlled by the Rad53 and Dun1 sensor kinases in budding yeast (reviewed in Barnum and O'Connell, 2014). The following genes are known to be involved in the coordination of the DNA damage checkpoints: *RAD9, RAD17, RAD24, MEC3, DDC1, MEC1,* and *RAD53* (Weinert et al., 1994; Weinert and Hartwell, 1988; Longhese et al., 1997; Allen et al., 1994; reviewed in Rhind and Russell, 1988). *RAD17, RAD24, MEC3,* and *DDC1* are referred to as the *RAD24* epistasis group and, in conjunction with *RAD9, MEC1,* and *RAD53,* constitute the group of genes whose gene products are required for the metaphase checkpoint in budding yeast, while only *MEC1* and *RAD53* are required for the S/M checkpoint (Weinert et al., 1994; Weinert and Hartwell, 1988; Longhese et al., 1997; Allen et al., 1994; reviewed in Rhind and Russell, 1998). *MEC1* and *RAD53,* essential genes required for the S/M checkpoint and the metaphase checkpoint, slow entry into mitosis when the S phase is inhibited for the S/M checkpoint and mediate signal transduction pathways for other DNA damage checkpoints (reviewed in Longhese et al., 1997). The non-essential genes, *RAD9* and the *RAD24* epistasis group, contribute to all other known DNA damage checkpoints except the S/M checkpoint (reviewed in Longhese et al., 1997).

1.2 Forkhead-associated Domains

Forkhead-associated (FHA) domains have historically been studied for the purpose of evaluating protein-protein interactions established between FHA domain-containing proteins and their binding partners via phosphorylated threonine residue-based recognition of ligands by the phosphothreonine-binding site of the FHA domain (reviewed in Mahajan et al., 2008). However, recent research has identified a novel method of FHA domain ligand recognition that does not rely on this canonical method of phosphothreonine motif binding (Matthews et al., 2014).

1.2.1 FHA Domain Discovery and Characteristics

During a 1995 bioinformatics-based study of the family of forkhead transcription factors, the Forkhead-associated (FHA) domain was discovered (Hofmann and Bucher, 1995). FHA domains have since been identified in over 2000 proteins, both eukaryotic and prokaryotic, commonly functioning as regulatory proteins, kinases, phosphatases, or transcription factors (Hofmann and Bucher, 1995; Mahajan et al., 2008; reviewed in Mohammad and Yaffe, 2009). The FHA domain is currently the only known protein-protein interaction motif that specifically recognizes phosphorylated threonine (pThr) residues, using the canonical pThr-binding site located on an apical surface of the domain, and will often do so via the recognition of a pattern in the residues flanking the phosphorylated threonine residue (reviewed in Mahajan et al., 2008). Little amino acid sequence homology exists between the large number of known FHA domains; however, they do exhibit structural homology (reviewed in Mahajan et al., 2008). In general, FHA domains are 80-100 amino acids in length and fold into two beta sheets, forming an 11-stranded beta sandwich with connecting coiled loops (Durocher and Jackson, 2002; Mahajan et al., 2008; reviewed in Mohammad and Yaffe, 2009). FHA domains and the proteins in which they are found often have important roles relevant to human diseases, especially those that feature DNA damage responses, abnormal cell growth, and/or impaired cell cycle regulation (Mahajan et al., 2008).

1.2.2 Non-canonical FHA Domain Lateral Surface Interaction Patch Identification and Characterization

RADiation sensitive (Rad53) is a budding yeast cell cycle checkpoint kinase often used to study DNA damage-based checkpoint signalling (Shirahige et al., 1998; reviewed in Durocher and Jackson, 2002). One heavily studied pathway in yeast is that of DNA replication initiation and checkpoint activation (Shirahige et al., 1998). In this pathway, Rad53 acts in conjunction with the Dbf4-dependent kinase (DDK) to regulate the firing of licensed origins of replication during replication initiation (Shirahige et al., 1998; Duncker et al., 2002; reviewed in Matthews et al., 2012). DDK is a complex that consists of the yeast proteins Cdc7 and Dbf4 which function as the kinase and regulatory subunits, respectively (reviewed in Matthews et al., 2012 and Matthews et al., 2014). DDK-dependent phosphorylation of proteins located at licensed origins triggers DNA replication, whereas activated Rad53 effector kinase delays the entry of cells into the mitosis phase of the cell cycle in response to genotoxic stress (reviewed in Matthews et al., 2012). A unique feature of Rad53 is its possession of two FHA domains, FHA1 and FHA2 (reviewed in Duncker et al., 2002). However, through studying the interaction between Rad53 and one of its ligands, Dbf4, it was determined that the Rad53 and Dbf4 interaction relies primarily on FHA1 (Duncker et al., 2002).

While characterizing the minimal region of Dbf4 required for its interaction with the FHA1 domain of Rad53, a BRCA1 C-terminal (BRCT) domain housing an additional alpha-helix within its core domain, referred to as an H-BRCT domain, was found within the N-terminal region of Dbf4 (Matthews et al., 2012). This H-BRCT domain was then analyzed using site-directed mutagenesis and yeast two-hybrid assays to determine the phosphoepitope that was expected to be bound by the canonical pThr-binding site of the Rad53 FHA1 domain (Matthews et al., 2014). However, individual mutagenesis of each of the threonine residues within the H-BRCT domain of Dbf4 was not able to disrupt the interaction between the H-BRCT domain and FHA1 (Matthews et al., 2014). As a result, the presence of an alternative interface

for the Rad53-Dbf4 interaction was hypothesized (Matthews et al., 2014). Via the use of nuclear magnetic resonance, bioinformatics and yeast two-hybrid analysis, a set of conserved residues located on the lateral surface of the Rad53 FHA1 domain was found to mediate the Rad53-Dbf4 interaction (Matthews et al., 2014). This discovery has expanded the scope of studying FHA domain-based protein-protein interactions, introducing the potential for discovering novel protein-protein interactions that may have been previously overlooked by studies that focused solely on the canonical pThr-binding site (Matthews et al., 2014).

1.3 DNA damage UNinducible (DUN1)

DNA damage UNinducible (DUN1) is a non-essential budding yeast gene that codes for the Dun1 checkpoint kinase, a protein involved in signal transduction pathways for DNA damage and replication stress as well as natural progression through S phase (reviewed in Tsaponina et al., 2011). Dun1 is 513 amino acids long and includes two functional domains, the N-terminal FHA domain and the C-terminal kinase domain (reviewed in Sanvisens et al., 2016; Figure 1.3). The primary function of Dun1 is to regulate the levels of deoxyribonucleoside triphosphates (dNTPs), the fundamental building blocks of DNA, via the transcriptional, spatial, and functional regulation of ribonucleotide reductase (RNR), the tetrameric protein complex responsible for catalyzing the dNTP synthesis rate-limiting step of converting ribonucleoside diphosphates into their deoxy form (reviewed in Chen et al., 2007, Sanvisens et al., 2016, Yoshitani et al., 2008, Lee and Elledge, 2006 and Zhao and Rothstein, 2002; Figure 1.4).

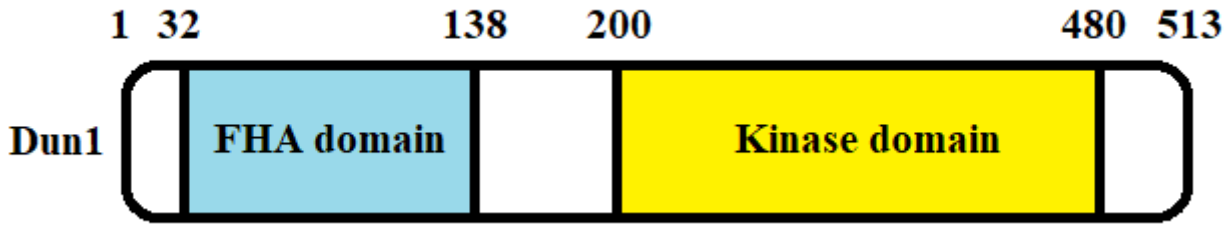

Figure 1.3: Structured Regions and Positions of Dun1

Dun1 schematic diagram showing the positions and order of Dun1 structured regions. Numbers above represent amino acid positions from N-to C-terminus (adapted from Sanvisens et al., 2016).

There are four genes that encode budding yeast RNR, *RNR1, RNR2, RNR3,* and *RNR4*, but only *RNR1, RNR2,* and *RNR4* are essential for the formation of the subunits of functional RNR (reviewed in Tsaponina et al., 2011). The function of *RNR3,* an *RNR1* isoform, remains unclear (reviewed in Tsaponina et al., 2011). RNR consists of two large subunits, a homodimer of Rnr1, and two small subunits, a heterodimer of Rnr2 and Rnr4 (reviewed in Sanvisens et al., 2016, Lee and Elledge, 2006 and Yoshitani et al., 2008; Figure 1.4). The small subunits of RNR have a di-iron centre that holds and maintains a tyrosyl radical that is essential for the catalytic biochemical activity of the enzyme, and the large subunits have the catalytic and allosteric sites (reviewed in Lee and Elledge, 2006 and Sanvisens et al., 2014).

In response to DNA damage, replication stress, or when cells enter S phase, the Mec1/Rad53/Dun1 kinase cascade leads to the activation of the RNR enzyme (reviewed in Sanvisens et al., 2014, Chen et al., 2007, Sanvisens et al., 2016, Yoshitani et al., 2008 and Zhao and Rothstein, 2002). Activated Mec1 sensor kinase leads to the phosphorylation of Rad53 and the FHA domain of Dun1 utilizes its unique capability of recognizing a di-phosphothreonine motif in hyperphosphorylated Rad53 to establish its Rad53-mediated phosphorylation and activation, leading to the Dun1-dependent phosphorylation of downstream targets essential to Dun1 function (Lee et al., 2003; Lee et al., 2008b; Bashkirov et al., 2003; reviewed in Sanvisens et al., 2014). There are four protein-coding genes whose products function downstream of Dun1 in the budding yeast dNTP regulation pathway (reviewed in

Sanvisens et al., 2016; Figure 1.4). *WTM1* encodes a protein that anchors Rnr2 and Rnr4 to the nucleus, *SML1* encodes an inhibitor of RNR large subunit activity, *DIF1* encodes a protein responsible for the nuclear import of the Rnr2 and Rnr4 subunits, and *CRT1* encodes a transcriptional repressor for the Rnr2 and Rnr4 genes (reviewed in Sanvisens et al., 2016). Mec1/Rad53 phosphorylation-dependent activation of Dun1 results in the phosphorylation of Crt1, phosphorylation and degradation of Dif1 and Sml1, and the hypothesized phosphorylation of Wtm1 resulting in the release of Rnr2 and Rnr4 transcriptional repression, the release of Rnr activity inhibition, and the re-localization of Rnr2 and Rnr4 to the cytoplasm in order to form a functional RNR holoenzyme (Sanvisens et al., 2016; Figure 1.4).

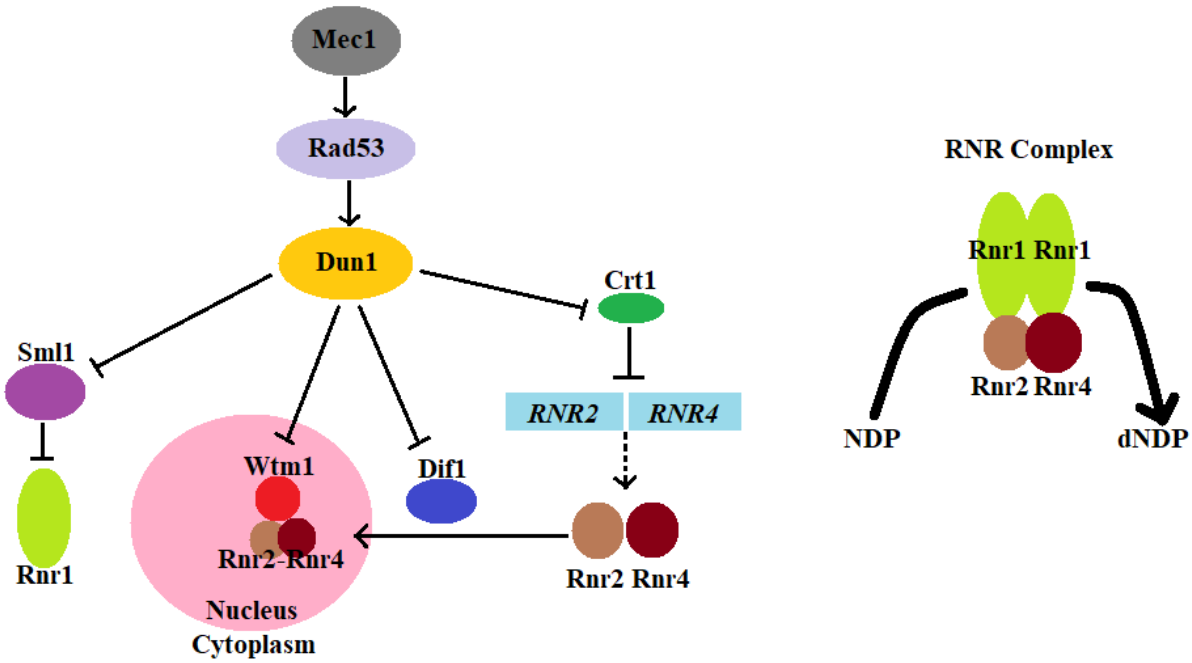

Figure 1.4: Dun1 and the dNTP Regulation Pathway

Depiction of the Dun1 dNTP regulation pathway, illustrating the role of the activated Dun1 kinase, the proteins responsible for activating Dun1 kinase, and the proteins that are regulated by activated Dun1 in the dNTP regulation pathway (adapted from Sanvisens et al., 2016).

Wtm1 is a member of the WTM (WD repeat-containing Transcriptional Modulator) family of WD40-repeat proteins, a protein family that exhibits many diverse functions such as transcriptional control, signal transduction, autophagy and apoptosis (Pemberton and Blobel, 1997; reviewed in Lee and

Elledge, 2006). *WTM1*, *WTM2*, and *WTM3*, identified in the *WTM* gene family in budding yeast, are homologs that likely arose due to gene duplication and all three of them encode nuclear proteins (Pemberton and Blobel, 1997; Huh et al., 2003; reviewed in Lee and Elledge, 2006). Of the three genes, *WTM3* is the most divergent (Pemberton and Blobel, 1997). Both *WTM1* and *WTM2* encode proteins that bind to themselves as well as each other (Pemberton and Blobel, 1997) and despite the fact that both Wtm1 and Wtm2 are able to bind to the Rnr2 and Rnr4 subunits of RNR, it is Wtm1 that is responsible for the localization of the Rnr2 and Rnr4 subunits via its action as a nuclear anchor (Lee and Elledge, 2006). The association of Rnr2-Rnr4 subunits with the Wtm1 nuclear protein holds Rnr2 and Rnr4 in the nucleus (Lee and Elledge, 2006; reviewed in Sanvisens et al., 2016). Proposed phosphorylation of Wtm1 by Dun1 in response to DNA damage disrupts the association between Wtm1 and Rnr2-Rnr4 releasing Rnr2-Rnr4 from the nucleus to the cytoplasm where its association with Rnr1 subunits form a functional RNR holoenzyme that can catalyze dNTP synthesis (Lee and Elledge, 2006; reviewed in Sanvisens et al., 2016).

Suppressor of mec1 lethality (SML1), named after the observation that the addition of a *sml1* mutation could restore viability to lethal *mec1* mutants, encodes a small and largely disordered suppressor protein that negatively affects dNTP synthesis by binding to the Rnr1 subunit and inhibiting its activity (Zhao et al., 1998, reviewed in Andreson et al., 2010). Mec1 and Rad53 are required to remove that inhibition during S phase in order to facilitate DNA replication (Zhao et al., 1998). The carboxyl terminus of Rnr1 associates with the amino terminus of Rnr1 in order to regenerate the active site located on the amino terminus using a cysteine pair located on the carboxyl terminus (Zhao et al., 1998, 2000; Chabes et al., 1999; Zhang et al., 2007; reviewed in Sanvisens et al., 2014). Sml1 competes with the carboxyl terminus for an association with the amino terminus and in doing so hinders Rnr1 active site regeneration, preventing the catalytic activity of RNR (Zhao et al., 1998, 2000; Chabes et al., 1999; Zhang et al., 2007; reviewed in Sanvisens et al., 2014). Sml1 phosphorylation at serine residues within its Sml domain by the Mec1/Rad53/Dun1 kinase cascade results in a conformational change in Sml1 that causes it to dissociate

from Rnr1 (Andreson et al., 2010). Phosphorylated Sml1 is then recognized by the Rad6-Ubr2-Mub1 E2/E3 ligase complex, ubiquitinylated, and targeted for degradation by the 26S proteosome, allowing the Rnr1 active site to be regenerated and dNTPs to be synthesized (Andreson et al., 2010).

Damage-regulated Import Facilitator (DIF1) is a paralog of *SML1* (Lee et al., 2008a). *DIF1, SML1,* and another yeast gene *HUG1* arose following the duplication and divergence of an ancestral gene, resulting in *DIF1* on chromosome XII and both *SML1* and *HUG1* on chromosome XIII (Lee et al., 2008a). Similar to *SML1, DIF1* encodes a small and largely disordered protein (Lee et al., 2008a). Dif1 contributes to dNTP regulation during S-phase in a cell cycle-dependent manner when Dif1 levels peak towards the end of S phase (Lee et al., 2008a; reviewed in Sanvisens et al., 2016). Dif1 shares a conserved domain with Sml1, referred to as the Sml domain, and another conserved domain with Hug1, referred to as the Hug domain (Lee et al., 2008a). Dif1 imports the Rnr2-Rnr4 small subunits from the cytoplasm to the nucleus via an association between its Hug domain and the Rnr2-Rnr4 small subunits (Lee et al., 2008a). Hypothetically, Dif1 carries out its import function either by acting as an adaptor or activating a dormant nuclear localization signal on the Rnr2-Rnr4 complex (Lee et al., 2008a). During S phase and in response to DNA damage when a rise in dNTP levels is required, Dif1 is phosphorylated and degraded in order to prevent the import of Rnr2-Rnr4 subunits from the cytoplasm to the nucleus (Lee et al., 2008a; reviewed in Sanvisens et al., 2016). The Sml domain of Dif1 is a phosphodegron and the direct phosphorylation of serine residues within the Sml domain by Dun1 results in the degradation of Dif1 and the maintenance of Rnr2-Rnr4 localization in the cytoplasm where it can associate with Rnr1 subunits to form a functional RNR holoenzyme that can synthesize dNTPs to increase dNTP levels (Lee et al., 2008a; reviewed in Sanvisens et al., 2016).

Constitutive RNR Transcription (CRT1) is one of many genes that encode regulators of DNA damage inducibility (Huang et al., 1998). *CRT1* encodes a transcriptional repressor specifically responsible for the repression of the *RNR2, RNR3,* and *RNR4* genes (Huang et al., 1998). Crt1 mediates repression via the recruitment of two general repressors, Tup1 and Ssn6, to the promoters of target genes

(Huang and Elledge, 1997; Huang et al., 1998; reviewed in Tsaponina et al., 2011). *RNR2* and *RNR4* repression specifically prevents RNR holoenzyme formation and thereby its function, however, Dun1-dependent phosphorylation of Crt1 prevents the transcriptional repression of *RNR2, RNR3,* and *RNR4* allowing Rnr2 and Rnr4 production and formation of the RNR holoenzyme for dNTP synthesis (Huang and Elledge, 1997; Huang et al., 1998; reviewed in Tsaponina et al., 2011 and Sanvisens et al., 2016).

1.4 Research Objectives

The imperative question, following the discovery of the non-canonical FHA domain lateral surface interaction patch on the Rad53 FHA1 domain and its importance to the interaction between Rad53 and Dbf4, was whether or not other FHA domain-containing proteins possess a non-canonical FHA domain lateral surface interaction patch and, if so, to what extent does it contributes to both previously identified and novel protein-protein interactions. Previous work in the Duncker lab demonstrated that mutations of the non-canonical FHA domain lateral surface interaction patch or the canonical pThr-binding site of the Dun1 FHA domain were sufficient to reduce the interaction between the Dun1 FHA domain and Sml1, only mutation of the pThr-binding site disrupted the interaction between the Dun1 FHA domain and Rad53, but that neither mutation of the Dun1 pThr-binding site nor of the lateral surface interaction patch were sufficient to disrupt the interaction between the Dun1 FHA with Dif1 (Robertson, 2015; Guitor, 2016). Additionally, yeast two-hybrid analysis of the Dun1 FHA domain and Crt1 suggested a lack of a protein-protein interaction (Guitor, 2016). As a result, the objective of the research presented in this thesis was to evaluate the contribution of the non-canonical FHA domain lateral surface interaction patch identified on the Dun1 FHA domain, compared to that of the canonical pThr-binding site, to protein-protein interactions involved in dNTP regulation in budding yeast. This objective was executed via the use of (1) yeast two-hybrid assays to confirm Dun1 ligands, (2) bioinformatics, site-directed mutagenesis and yeast two-hybrid assays to evaluate the interaction abrogation of Dun1 FHA

domain lateral surface interaction patch mutants compared to pThr-binding site mutants with Dun1 ligands, and (3) spot plate assays to assess the genotoxic sensitivity of Dun1 FHA mutants.

Chapter 2

Materials and Methods

2.1 Yeast Strains

The following yeast strains were used for genomic DNA isolation, yeast two-hybrid assays, and spot plate assays (Table 2.1).

Table 2.1: List of Yeast Strains

Strain	Genotype	Source
DY-1	*MAT**a**, ade2-1, can1-100, trp1-1, his3-11, ura3-1, leu2-3, leu2-112, pep4::LEU2*	(Duncker et al. 2002)
DY-30	*MAT**a**, his3Δ1, leu2Δ0, met15Δ0, ura3Δ0*	ATCC
DY-145	*MAT**a**, ade2-1, can1-100, his3-11,15, leu2-3, trp1-1, ura3-1, SML1::HIS3 RAD5*	(Tam et al. 2008)
DY-147	*MAT**a**, ade2-1, can1-100, his3-11,15, leu2-3, trp1-1, ura3-1, SML1::HIS3, RAD5, RAD53::URA3*	(Tam et al. 2008)
DY-351	*MAT**a**, his3Δ1, leu2Δ0, met15Δ0, ura3Δ0, Dun1Δ*	GE Healthcare

* The *rad53Δ* mutation is coupled to the *smlΔ* mutation in order to rescue *rad53Δ* lethality (reviewed in Dohrmann and Sclafani, 2006).

2.2 Genomic DNA Isolation

Genomic DNA was isolated from the DY-1 yeast strain for use as template DNA for most PCR reactions for plasmid construction. A working culture of DY-1, inoculated from a saturated culture grown for 2 days at 30°C, was grown to a concentration of ~ 1 x 10^7 cells/mL in 10 mL of YPD (10 % yeast extract, 20 % peptone, and 20 % dextrose) media. Cells were centrifuged at 4000 rotations-per-minute (rpm) for 5 minutes, re-suspended in 500 µL of sterile water and transferred to a sterile 2 mL screw-cap tube. Re-suspended cells were centrifuged for 10 seconds at maximum speed, the supernatant decanted, and then mixed at a low speed on a vortex to loosen the pellet. A 200 µL aliquot of 'genomic prep mix' (2% Triton X-100, 1% SDS, 100 mM NaCl, 10 mM Tris-Cl pH 8, and 1 mM EDTA) was added to the loosened pellet, followed by 200 µL of phenol:chloroform:isoamylalcohol (25:24:1) and 0.5 g of 0.5 mm

glass beads. All components were mixed for 3-4 minutes using a vortex and then 200 µL of 1X TE pH 8 was added and mixed. Following a 5 minute centrifugation at maximum speed, the top layer was transferred to a new sterile 1.5 mL tube with 1 mL of 100% room temperature ethanol and mixed by inversion. After another run of centrifugation for 2 minutes at maximum speed, the pellet was completely re-suspended in 0.4 mL of 1X TE pH 8 to which 10 µL of 10 mg/mL RNase A (Sigma) was added before incubating at 37°C for 10 minutes. After incubation, 10µL of 4 M ammonium acetate and 1 mL of room temperature 100% ethanol were added and mixed by inversion. After a 2 minute centrifugation, the supernatant was discarded and the pellet left to air dry before completely re-suspending the pellet in 50 µL of 1X TE pH 8. Genomic DNA was stored at -20°C.

2.3 Bioinformatics Analysis

Protein BLAST (BLASTp) searches were done using the full length amino acid sequence of Dun1 (S288C, Saccharomyces Genome Database, https://www.yeastgenome.org/locus/S000002259) as the input of a search against the non-redundant protein sequences (nr) database using the Position-Specific Iterated BLAST (PSI-BLAST) algorithm in order to identify Dun1 homologs (National Center for Biotechnology Information, NCBI). A selection of returned sequences with percentage identities of approximately 30% were used to generate a multiple sequence alignment (MSA) in the ClustalW format using the online MUltiple Sequence Comparison by Log-Expectation (MUSCLE) tool (European Molecular Biology Laboratory, EMBL-EBI). The MUSCLE-generated MSA file was examined using the Jalview software to identify and illustrate highly conserved residues within the in Dun1 FHA domain using amino acid percent identity beyond a threshold of 30% to colour the residues in accordance with their conservation for a range of blue for high conservation to white for low conservation (http://www.jalview.org/). Using the UCSF Chimera protein model analysis software and its Multi-Align viewer tool or the Consurf server (http://consurf.tau.ac.il/2016/), the MUSCLE-generated MSA was used to map the amino acid sequence conservation of Dun1 homologs to the Dun1 FHA domain model (PDB

template ID: 2JQJ) using colouration to depict the level of conservation ranging from red residues showing high conservation to blue residues showing low conservation. Chimera was also used to assess the orientation of the amino acid side chains for highly conserved residues in order to identify highly conserved surface residues that could contribute to protein-protein interaction surfaces for the canonical pThr-binding site or non-canonical FHA domain lateral surface interaction patch (https://www.cgl.ucsf.edu/chimera/download.html). The following table outlines the BLASTp query results listing the accession numbers, organisms, and the products of the associated genes (Table 2.2).

Table 2.2: Protein BLAST Query for Dun1 Homologs

Accession #	Organism	Product
NP_010182.1	Saccharomyces cerevisiae S288c	serine/threonine protein kinase DUN1
XP_018222985.1	Saccharomyces eubayanus	DUN1-like protein
XP_003675046.1	Naumovozyma castellii CBS 4309	hypothetical protein NCAS_0B05910
XP_003682860.1	Torulaspora delbrueckii	hypothetical protein TDEL_0G02820
XP_003668597.1	Naumovozyma dairenensis CBS 421	hypothetical protein NDAI_0B03190
XP_003959736.1	Kazachstania africana CBS 2517	hypothetical protein KAFR_0K02450
NP_985362.2	Eremothecium gossypii ATCC 10895	AFL188Cp
XP_001645503.1	Vanderwaltozyma polyspora DSM 70294	hypothetical protein Kpol_1004p19
XP_449096.1	Candida glabrata CBS 138	hypothetical protein
XP_003685041.1	Tetrapisispora phaffii CBS 4417	hypothetical protein TPHA_0C04570
XP_002494696.1	Zygosaccharomyces rouxii	ZYRO0A07546p
XP_003647177.1	Eremothecium cymbalariae DBVPG#7215	hypothetical protein Ecym_5624
XP_004179070.1	Tetrapisispora blattae CBS 6284	hypothetical protein TBLA_0B07330
XP_017988713.1	Eremothecium sinecaudum	HFL139Cp
XP_002999388.1	Kluyveromyces lactis NRRL Y-1140	hypothetical protein

*****Shading indicates the Dun1 protein sequence input for BLASTp search. Dun1 homologs selected for the Multiple Sequence Alignment (MSA) are not shaded.

2.4 Site-directed mutagenesis

Site-directed mutagenesis was used to generate mutations, primarily point mutations, within the *DUN1* coding sequence using the QuikChange II XL Site-Directed Mutagenesis Kit and its full protocol which is available online: http://www.agilent.com/cs/library/usermanuals/public/200523.pdf (Agilent Technologies). Mutagenic primers were designed using the QuikChange Site-Directed Mutagenesis online interface (https://www.genomics.agilent.com/primerDesignProgram.jsp) and then utilized during PCR to remove or replace the desired nucleotide(s). The PCR product was digested with provided Dpn1 restriction endonuclease in order to degrade parental copies of the plasmid containing the gene to be mutagenized and then the product was transformed into the provided XL-10 Gold Ultracompetent cells and plated on Luria-Bertani (LB) agar (1% NaCl, 1% tryptone, 0.5% yeast extract, and 2.4% agar) containing the antibiotic ampicillin (BioShop). Colony PCR was used to confirm colonies that maintained the integrity of both the insert and vector and then plasmid DNA from plasmid preps of 4 positive clones was sent for sequencing at the Robarts Sequencing Facility.

2.5 **Plasmid Construction**

Plasmids were constructed using either the pEG202, pJG4-6, or pRS315 vectors (Ausubel et al., 1994; Gyuris et al., 1993, reviewed in Duncker et al., 2002; Dobson et al., 2005). Plasmid constructs made with the pEG202 and pJG4-6 vectors were designed for use in yeast two-hybrid assays, and constructs made with the pRS315 vector were used for spot plate assays. The pEG202 and pJG4-6 vectors are referred to as the bait and prey vectors in the context of yeast two-hybrid assays (Ausubel et al., 1994; Gyuris et al., 1993, reviewed in Duncker et al., 2002). In addition to traditional cloning vector features, the bait and prey vectors contain a selectable marker for the biosynthesis of histidine and tryptophan, respectively, as well as the coding sequence of the DNA binding domain and transcriptional activation domain of the transcription factor for the *LacZ* reporter located on the pSH18-34 reporter plasmid utilized during yeast two-hybrid assays (Ausubel et al., 1994; Gyuris et al., 1994). In addition to other cloning

vector traditional features, the pSH18-34 plasmid contains a selectable marker for the biosynthesis of uracil (Ausubel et al., 1994; Gyuris et al., 1994). The pRS315 vector, YCp or yeast centromeric plasmid contains a selectable marker for the biosynthesis of leucine amongst its other traditional cloning vector features. Due to the incorporation of yeast centromeric sequence within the plasmid, pRS315 is maintained in yeast cells with a low copy number of usually 1-2 copies per cell (Clarke and Carbon, 1980; Ishii et al., 2009; Stearns et al., 1990). This feature was exploited in order to allow the expression of gene(s) of interest at a level approximating that of genomic DNA.

The protein coding sequence of *DUN1* for the region of the FHA domain, amino acids 21-145, was previously cloned into the pJG4-6 vector in the Duncker Lab. The following Dun1 FHA domain mutants were generated via site-directed mutagenesis using the pre-existing Dun1 FHA domain construct as a template: pJG4-6 *dun1-R60A-fha,* pJG4-6 *dun1-N108A-fha,* pJG4-6 *dun1-K136A-fha,* pJG4-6 *dun1-2M-fha,* pJG4-6 *dun1-4M-fha,* pJG4-6 *dun1-N121A-fha,* pJG4-6 *dun1-L134A-fha,* and pJG4-6 *dun1-KRA-fha.* The full-length coding sequence for *DUN1* was amplified from DY-1 genomic DNA via the Polymerase Chain Reaction (PCR) using a commercially available High-Fidelity PCR kit (Roche) for the construction of the pJG4-6 *DUN1* plasmid. PCR products were purified using a commercial PCR clean up kit that was also used for the clean-up of EcoRI and ApaI forward and reverse restriction enzyme digested PCR products and vectors (Geneaid). All restriction enzymes were purchased from Thermo Fisher Scientific and their sequences were incorporated into the design of the primers used for PCR amplification. Ligation was completed using a T4 DNA ligase kit (BioBasic), and the ligated product was transformed into calcium-chloride competent DH5α *Escherichia coli (E. coli)* cells grown and plated on LB media (1% NaCl, 1% tryptone, 0.5% yeast extract, and 2.4% agar) containing the antibiotic ampicillin (BioShop). Colony PCR was performed using a commercial colony PCR kit (New England Biolabs). Plasmid DNA was isolated from saturated overnight cultures of DH5α for positive colonies using a commercial plasmid prep kit (Geneaid). The full protocol for plasmid DNA purification is available online: http://www.geneaid.com/sites/default/files/PD13.pdf. Plasmid DNA from 2-4 positive clones was

sent for sequencing of the full length of the insert at the Robarts Sequencing Facility to ensure the fidelity of the cloned PCR product. Site-directed mutagenesis of the full-length *DUN1* prey construct generated the following Dun1 mutants in the context of full-length Dun1: pJG4-6 *dun1-ΔFHA,* pJG4-6 *dun1-N108A,* pJG4-6 *dun1-K136A,* pJG4-6 *dun1-2M,* pJG4-6 *dun1-4M,* pJG4-6 *dun1-KRA,* pJG4-6 *dun1-N121A,* pJG4-6 *dun1-L134A,* pJG4-6 *dun1-D328A,* pJG4-6 *dun1-T380A,* and pJG4-6 *dun1-R60A.*

The full-length *DUN1* coding sequence along with its native promoter, 600 base pairs upstream of the coding sequence, was amplified from DY-1 genomic DNA as described previously for the pJG4-6 *DUN1* construct, cloned into a pCM190-myc13 vector and then moved, with or without the myc13 tag, into the pRS315 plasmid using BamHI and NotI forward and reverse restriction enzymes in order to generate the pRS315 *DUN1* construct. Site-directed mutagenesis of the *DUN1* construct generated the following mutants in the context of full-length *DUN1:* pRS315 *dun1-N108A,* pRS315 *dun1-K136A,* pRS315 *dun1-2M,* pRS315 *dun1-4M,* pRS315 *dun1-KRA,* pRS315 *dun1-ΔFHA,* pRS315 *dun1-R60A,* pRS315 *dun1-N121A,* and pRS315 *dun1-L134A.*

All Dun1 constructs generated within the pJG4-6 vector were used to create the same constructs in the pEG202 vector via EcoRI and XhoI forward and reverse restriction enzyme digests of the pJG4-6 constructs and ligation into the pEG202 vector: pEG202 *DUN1-FHA,* pEG202 *dun1-R60A-fha,* pEG202 *dun1-N108A-fha,* pEG202 *dun1-K136A-fha,* pEG202 *dun1-2M-fha,* pEG202 *dun1-4M-fha,* pEG202 *dun1-N121A-fha,* pEG202 *dun1-L134A-fha,* pEG202 *dun1-KRA-fha,* pEG202 *DUN1,* pEG202 *dun1-ΔFHA,* pEG202 *dun1-N108A,* pEG202 *dun1-K136A,* pEG202 *dun1-2M,* pEG202 *dun1-4M,* pEG202 *dun1-KRA,* pEG202 *dun1-N121A,* pEG202 *dun1-L134A,* and pEG202 *dun1-R60A.*

The full-length coding sequences of *DIF1, SML1, CRT1,* and *RAD53* had already been cloned into the pEG202 vector along with full-length *RAD53* in the pJG4-6 vector by members of the Duncker Lab. The full-length coding sequence of *WTM1* was amplified from DY-1 genomic DNA and cloned into the pEG202 vector as described previously for the pJG4-6 *DUN1* construct, and then the full-length coding sequences of *SML1, CRT1,* and *WTM1* were digested from the pEG202 vector using the EcoRI

forward and XhoI reverse restriction enzymes and inserted into the pJG4-6 vector to generate the following constructs: pJG4-6 *SML1*, pJG4-6 *CRT1*, and pJG4-6 *WTM1*.

2.6 Yeast Transformation

Plasmid DNA containing the protein coding sequence for genes of interest was transformed into the DY-1 yeast strain pre-transformed with the pSH18-34 reporter plasmid for yeast two-hybrid assays or the DY-351 yeast strain for spot plate assays. A working culture of the appropriate yeast strain was grown to a concentration of ~ 1 x 10^7 cells/mL in 10 mL of either Synthetic Complete (SC) media (0.17 % yeast nitrogen base, 0.5 % ammonium sulfate, 2 % glucose, 1X amino acid mix) lacking uracil for the selection of the pSH18-34 reporter plasmid or YPD (10 % yeast extract, 20 % peptone, 20 % dextrose). Working cultures were centrifuged for 5 minutes at 4000 rpm, resuspended in 1X Tris-EDTA (TE) solution pH 8.0, centrifuged again, resuspended in 200 µL of Lithium acetate/TE solution (100 mM lithium acetate, 2.5 mL 1X TE), and then held at room temperature for 10 minutes. Approximately 0.4 µg of plasmid DNA was added to 100 µL of the yeast suspension mix along with 100 µg of salmon sperm DNA, and then 300 µL of Lithium acetate/TE/PEG4000 solution (100 mM Lithium acetate, 2 g polyethylene glycol 4000, 0.5 mL 10X TE) was added. The solution was incubated at 30°C for 30 minutes before 40 µL of dimethylsulfoxide (DMSO) was added. Cells were heat shocked at 42°C for 7 minutes, held on ice for 2 minutes and then plated on selective media and grown for 2-3 days.

2.7 Yeast two-Hybrid Assay

This technique was performed as outlined previously (Duncker et al., 2002). DY-1 yeast cells pre-transformed with the pSH18-34 lacZ reporter plasmid were transformed with a pEG202-derived bait construct and a pJG4-6-derived prey construct (Ausubel et al., 1994; Gyuris et al., 1993; reviewed in Duncker et al., 2002). A physical interaction between the bait and prey proteins during the assay would bring the DNA binding domain, fused to the gene of interest expressed from the bait vector, and the

transcriptional activation domain, fused to the gene of interest expressed from the prey vector, into close enough proximity to form an active transcription factor for the *LacZ* reporter gene located on the pSH18-34 plasmid (shown in Figure 2.1). The *LacZ* gene encodes β-galactosidase, an enzyme that produces a yellow ortho-nitrophenyl (ONP) product from the breakdown of the ortho-Nitrophenyl-β-galactoside (ONPG) substrate. The level of β-galactosidase activity indicates the strength of a protein-protein interaction and is determined via the following calculation: β-galactosidase activity = 1000 x A420/ (t x V x A600), where A420 and A600 are absorbance readings at 420 nm for the produced ortho-nitrophenyl (ONP) from the reaction and 600 nm for the yeast culture, t is the time for the reaction, and V is the volume in millilitres of culture needed for 5 x 10^6 cells.

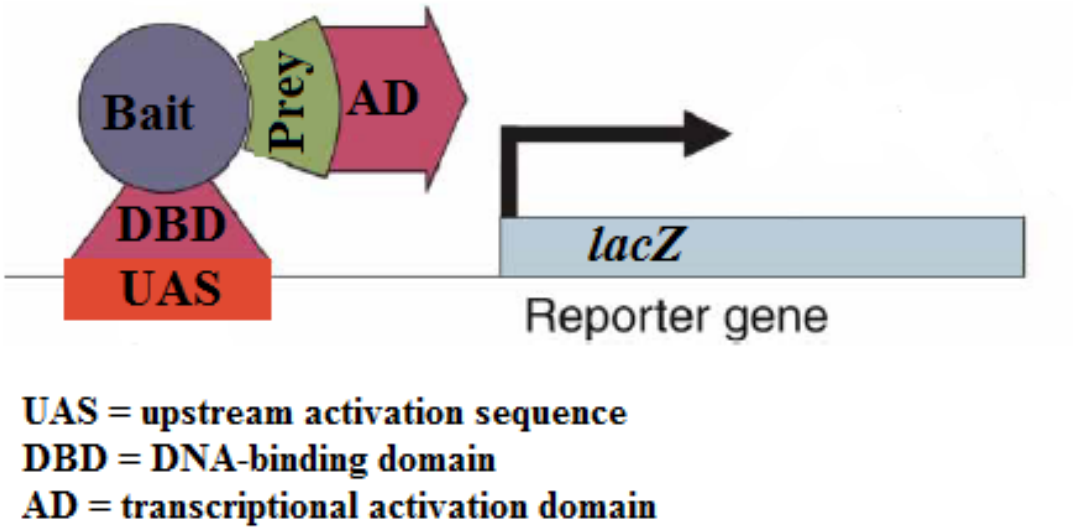

Figure 2.1: Schematic Diagram of the Yeast two-hybrid Assay

Yeast two-hybrid assay and the main mechanistic features. The reporter gene and its upstream activation sequence, located on the pSH18-34 plasmid, are used to detect a protein-protein interaction between the bait and prey proteins. The bait vector has the DNA binding domain and the prey vector has the transcriptional activation domain. An interaction between the bait and the prey proteins bring the two domains of the transcription factor into close enough proximity to form an active transcription factor for the reporter gene (adapted from Lehne and Schlitt, 2009).

Yeast cultures were grown in 10 mL of SC media without uracil, histidine, or tryptophan to a concentration of ~ 1.0 x 10^7 cells/mL. Following centrifugation for 5 minutes at 4000 rpm, cells were washed in sterile water and incubated for six hours at 30°C and a speed of 200 rpm in 20 mL of Galactose/Raffinose media (0.17 % yeast nitrogen base, 0.5 % ammonium sulfate, 2% galactose, 1% raffinose) lacking uracil, histidine, and tryptophan in order to induce recombinant protein expression from the prey vector. Following induction, cells were counted using a haemocytometer and then ~ 5 x 10^6 cells were harvested for the assay. The cells were centrifuged for 10 minutes at 16X gravity (g) and then resuspended in 0.5 mL of Z buffer (60 mM Na_2HPO_4, 40 mM NaH_2PO_4, 10 mM KCl, 1 mM $MgSO_4$, and 0.05M β mercaptoethanol). Using a P200 micropipette, 2 drops of chloroform and 1 drop of 0.1% sodium dodecyl sulfate (SDS) were added to the resuspended cells which were then vortexed at maximum speed for 10 seconds and then incubated for 5 minutes at 28°C. After the 5 minute incubation, 100 µL of ONPG (4 mg/mL in 0.1 M potassium phosphate buffer, pH 7, Sigma) was added to begin the β-galactosidase reaction. Based on the appearance of a yellow colour in the reaction solution, 250 µL of 1 M Na_2CO_3 (BioShop) was then added to stop the reaction. After a final centrifugation of 10 minutes at 16X g, the OD_{600} and OD_{420} were measured in order to calculate the β-galactosidase activity.

2.8 Yeast Whole Cell Extract and Western Blotting

In order to verify appropriate protein expression, yeast whole cell extracts (WCE) were generated for Western blotting. Approximately 20 mL of yeast culture (~ 1.0 X 10^7 cells/mL) were spun down for 5 minutes at 4000 rpm to pellet cells, resuspended in 300 µL of lysis buffer (10 mM Tris-HCl pH 8.0, 140 mM NaCl, 1% Triton X-100, 1 mM EDTA, 100 µL of Fisher HALT! protease inhibitor and 1 mM PMSF) and added to a 2 mL tube with 0.3 g of 0.5 mm glass beads before subjecting the samples to lysis at 4°C via the use of the Biospec Mini Bead-Beater for eight cycles of 30 seconds of agitation and 30 seconds of rest on ice. A total of 105 µL of supernatant (whole cell extract) was collected following the centrifugation of lysed cells for 30 seconds at 13, 200 rpm in 4°C: 5 µL for the Bradford Assay and 100

µL for the SDS-PAGE. The Bio-Rad Bradford Assay was used to determine the protein concentrations of each sample (Bio-Rad). Protein extracts were mixed with loading buffer (60% 4X buffer [15% SDS, 40% glycerol, and 166 mM Tris base], 0.26 M DTT, 7% bromophenol blue) at a volume of one-half that of the extract and then boiled for 10 minutes before loading 30 - 50 µg of protein onto SDS polyacrylamide gels (10 % resolving gel and 5% stacking gel). After electrophoresis, proteins were transferred from the gel to a nitrocellulose membrane using a wet transfer method (200 mM glycine, 25 mM Tris-base, 20 % methanol, 0.054% SDS for the transfer buffer). Membranes were pre-stained with 0.1% Ponceau S, imaged using an Epson scanner (any good quality scanner can be used), and then de-stained with 1X TEN + T (20 mM Tris-HCl, 1 mM EDTA, 0.14 NaCl, 0.05% Tween 20) before detection with antibodies (Table 2.3). Antibody incubations were performed for 1-2 hours after 1 hour blocking in 1X TEN + T with 5% skim milk powder. Three 10 minute washes were done using 1X TEN + T after each antibody exposure and images were taken with a Pharos FX Plus imager (Bio-Rad).

Table 2.3: List of Antibodies

Antibody	Dilution	Source
Anti-HA (mouse monoclonal) - pJG4-6	0.75:5000 in 3% bovine serum albumin, BSA	Sigma
Anti-LexA (rabbit polyclonal) - pEG202	1:5000 in 3% BSA	Cedarlane
Anti-MYC (mouse monoclonal) - pRS315	1:5000 in 3% BSA	Sigma
AlexaFluor 488 anti-mouse	1:3000 in 5% skim milk	Invitrogen
AlexaFluor 647 anti-rabbit	1:3000 in 5% skim milk	Invitrogen

2.9 Spot Plate Assay

The spot-plate assay was used to determine the growth defects of yeast cells exposed to genotoxic stress under the circumstances of reduced or abolished interactions between Dun1 and other proteins involved in dNTP regulation: Rad53, Wtm1, Crt1, Dif1 and Sml1. Genotoxic agents used as stressors were intended to cause DNA damage, an inability to repair DNA damage, or impair DNA synthesis. A *DUN1* genomic knockout yeast strain, DY-351, purchased from GE Healthcare was used for yeast

transformation of full length Dun1 expression vectors. Using a sterile 60-well plate, three 1:10 dilutions were made from an initial dilution of 30 µL of saturated (~ 1 x 10^8 cells/mL) culture diluted in 270 µL of media. Aliquots of 5 µL of the four serial dilutions of yeast culture were plated onto 25 mL of solid agar, either synthetic complete (SC) lacking leucine or yeast peptone dextrose (YPD), containing various levels of genotoxic agents. Genotoxic agents were mixed into 25 mL aliquots of agar media prior to agar solidification. Genotoxic compounds used and their concentrations were as listed (Table 2.4).

Table 2.4: List of Genotoxic Agents

Genotoxic Agent	Action	Concentrations	Source
Hydroxyurea (HU)	dNTP pool depletion	20 mM - 200 mM	BioShop
Methane methylsulfonate (MMS)	DNA methylation	0.005% - 0.025%	Sigma
Bleomycin	DNA breakage	1 µg/mL - 5 µg/mL	Sigma
Phleomycin	DNA breakage	1 µg/mL - 5 µg/mL	Sigma
Camptothecin	DNA topoisomerase I inhibition	5 µM - 20 µM	Sigma

2.10 Statistical Analysis

The IBM SPSS software was used to ascertain the significance of the differences observed amongst yeast two-hybrid assay samples (https://www.ibm.com/analytics/data-science/predictive-analytics/spss-statistical-software). The One-way ANOVA test and its associated Tukey post-hoc test were used to determine whether or not the there were significant differences in the mean β-galactosidase activity for each yeast two-hybrid assay sample. The Levene's test and Kolmogorov-Smirov tests were used to assess the assumptions for homoscedasticity and normality, respectively, in order to confirm the appropriate use of the One-way ANOVA test. The acceptance threshold was set at 0.05. Means with different letters are significantly different (Tukey's HSD, $p < 0.05$).

Chapter 3

Dun1-Dif1 and Dun1-Sml1 interactions utilize the conserved non-canonical FHA domain lateral surface interaction patch

3.1 Introduction

A primary function of Dun1 is to increase the levels of dNTPs in a cell via its regulatory control of the transcription, localization, and function of the RNR enzyme subunits involved in the catalysis of the dNTP synthesis rate-limiting step (reviewed in Sanvisens et al., 2016). Mec1/Rad53-dependent phosphorylation and activation of Dun1 leads to the phosphorylation of downstream Dun1 targets: Wtm1, Sml1, Dif1, and Crt1, and the removal of their collective inhibition with respect to dNTP synthesis (Lee and Elledge, 2006; Andreson et al., 2010; Lee et al., 2008a; Huang and Elledge, 1997; Huang et al., 1998; reviewed in Sanvisens et al., 2016). The Dun1 protein consists of an N-terminal FHA domain and a C-terminal kinase domain that contribute to phosphoepitope recognition for ligand binding and phosphorylation of targets, respectively (reviewed in Sanvisens et al., 2016).

Mec1 sensor kinase activation results in the phosphorylation and activation of the Rad53 checkpoint kinase (reviewed in Lee et al., 2003). Dun1 recognition of hyperphosphorylated Rad53 via the Dun1 FHA di-phosphothreonine recognition motif allows for Rad53-dependent phosphorylation and activation of Dun1 (Lee et al., 2003; Lee et al., 2008b; Bashkirov et al., 2003; reviewed in Sanvisens et al., 2016). Considering the identification of the non-canonical FHA domain lateral surface interaction patch of the Rad53 FHA1 domain and its contribution to the FHA1 and H-BRCT interaction of Rad53 and Dbf4 (Matthews et al., 2014), the Dun1 FHA domain was assessed for the existence of a candidate conserved non-canonical FHA domain lateral surface interaction patch four years ago by Damir Mingaliev, an undergraduate student in the Duncker Lab. Using the candidate non-canonical FHA domain lateral surface interaction patch identified by Damir, Dun1 FHA domain ligands and binding patterns

were evaluated by Aaron Robertson and Allison Guitor, two other students in the Duncker lab. Using yeast two-hybrid assays, protein-protein interactions were observed between the Dun1 FHA domain and ligands: Sml1, Rad53 and Dif1, whereas an interaction between the Dun1 FHA domain and Crt1 was not observed (Robertson, 2015; Guitor, 2016). Yeast two-hybrid assays also showed the existence of different patterns in the association of the Dun1 FHA domain with its various ligands with respect to the requirement of the pThr-binding site and/or the lateral surface interaction patch (Robertson, 2015; Guitor, 2016).

The Dun1 FHA - Sml1 interaction appeared to require both the canonical and non-canonical interaction interfaces due to the observation that neither mutation of the pThr-binding site nor the lateral surface interaction patch led to complete abrogation of the interaction (Robertson, 2015). Analysis of the Dun1 FHA and Rad53 interaction showed that mutation of the canonical interface was able to completely disrupt the interaction whilst mutation of the non-canonical interface had no effect (Robertson, 2015). For the analysis of the Dun1 FHA - Dif1 interaction, mutation of the lateral surface interaction patch appeared to have no effect on the interaction, but mutation of the pThr-binding site appeared to increase the interaction strength (Guitor, 2016). An interaction between the Dun1 FHA domain and Wtm1 had yet to be tested, preliminary spot plate assays were not very conclusive, and the effects of a coupled pThr-binding site and lateral surface interaction patch mutant had not been assessed (Robertson, 2015).

3.2 Results

3.2.1 dNTP regulation pathway interactions exhibit different requirements

A prominent feature of the FHA domain is the recognition of phosphorylated threonine residues via the canonical pThr-binding site for the establishment of ligand recognition and binding for FHA domain-containing proteins (reviewed in Mahajan et al., 2008). The research presented in Matthews et al., 2014 initiated a quest for the discovery of other FHA domain-containing proteins besides Rad53 that possess a non-canonical FHA domain lateral surface interaction patch in addition to the canonical pThr-

binding site. The Multiple Sequence Alignment (MSA) of Dun1 homologs edited in Jalview illustrates the approximate regions of the canonical pThr-binding site and non-canonical FHA domain lateral surface interaction patch as well as the conservation of the residues encompassed within each area (Figure 3.1). Key residues previously identified as highly conserved residues of each area were used to demarcate those regions on the MSA (reviewed in Sanvisens et al., 2016; Robertson et al., 2015).

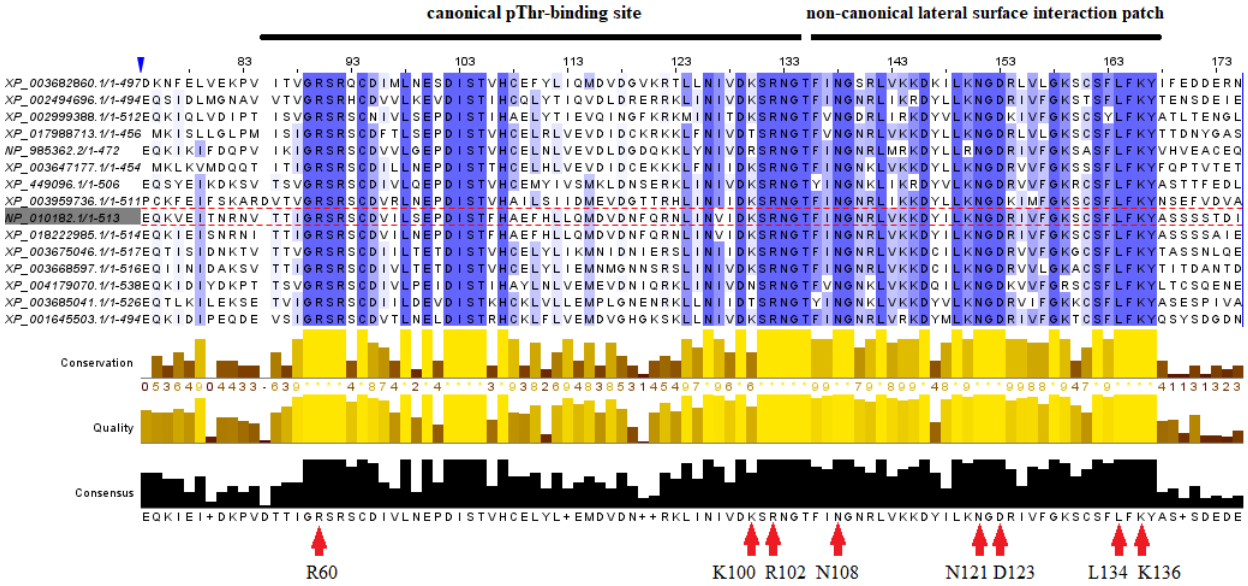

Figure 3.1: MUSCLE Multiple Sequence Alignment of Dun1 Homologs

A segment of the Multiple Sequence Alignment generated using the MUSCLE algorithm shows amino acid conservation for the Dun1 FHA domain, specifically the regions of the canonical pThr-binding site and non-canonical FHA domain lateral surface interaction patch. Key residues for the pThr-binding site and lateral surface patch were used to mark approximate borders for each region. Conservation was coloured using a range of blue (high conservation) to white (low conservation) based on a 30% percent identity threshold within the Jalview software. Single letters and numbers correspond with the amino acid letter code and the amino acid position with respect to *S. cerevisiae* Dun1.

The MUSCLE-generated MSA was then used to map amino acid sequence conservation to the surface of the Dun1 FHA domain model which illustrates the location of the pThr-binding site and the candidate lateral surface interaction patch (Figure 3.2). The apical region of the domain, known to house the pThr-binding site, is one large area of highly conserved residues. Another large area of highly conserved residues, representing the candidate non-canonical FHA domain lateral surface interaction

patch, can be seen on a lateral surface of the FHA domain. A small region of highly conserved residues near the apical region may or may not be a part of the canonical pThr-binding site.

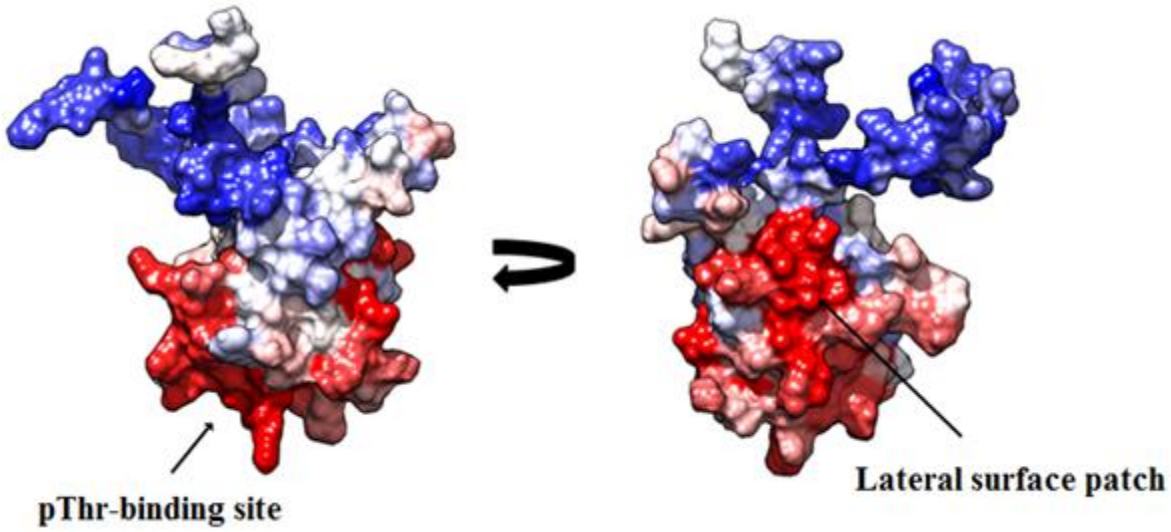

Figure 3.2: Conservation Mapping of the Dun1 FHA Domain

3-D surface model of the Dun1 FHA domain, amino acids 1-145, (PDB template ID: 2JQJ) showing amino acid conservation using colours ranging from red (high conservation) to blue (low conservation). Surface model shows the location of the canonical phosphothreonine-binding site and the candidate non-canonical FHA domain lateral surface interaction patch.

Preliminary re-assessment of previously confirmed Dun1 FHA domain binding partners revealed a lack of *RAD53* and *CRT1* expression from pEG202 two-hybrid bait vector constructs (data not shown), the same anomaly was observed with expression of *WTM1* from the pEG202 bait vector (data not shown). As a result *CRT1* and *WTM1* protein coding sequences were cloned into the pJG4-6 two-hybrid prey vector, a pJG4-6 *RAD53* construct was already available and functional in the Duncker Lab, where successful and consistent protein expression was recovered. Yeast two-hybrid assays and corresponding western blots were used to evaluate the necessity and/or sufficiency of the Dun1 FHA domain for interactions between Dun1 and the Rad53, Wtm1, and Crt1 ligands by comparing the interaction strengths of the ligands with full-length Dun1, just the FHA domain, or Dun1 without the FHA domain (Figure 3.3). Calculations of the mean β-galactosidase activity observed over three trials were illustrated in a

graph to show that the Dun1 FHA domain could interact with Rad53, Wtm1, and Crt1 (Figure 3.3A-C). Unlike the Dun1 FHA domain, neither full-length Dun1 nor Dun1 without its FHA domain were able to interact with Rad53, shown via the lack of β-galactosidase activity relative to the empty prey negative control (Figure 3.3A). Full-length Dun1 had twice as much β-galactosidase activity as the empty bait negative control for Wtm1 but only half of the β-galactosidase activity of the Dun1 FHA with Wtm1, indicating that only full-length Dun1 and just the FHA domain of Dun1 are capable of interacting with Wtm1. The lower β-galactosidase activity for full-length Dun1 is likely a result of lower full-length Dun1 protein expression (Figure 3.3B). For the analysis of Crt1, the empty bait negative control had an unexpectedly high signal for β-galactosidase activity that did not persist in samples that had Crt1 in the prey vector and a version of the Dun1 protein in the bait vector (Figure 3.3C). The lack of β-galactosidase activity for Crt1 with full-length Dun1 and Dun1 without the FHA domain indicates a lack of an observable interaction between Crt1 with full-length Dun1 and with Dun1 without the FHA domain (Figure 3.3C). The corresponding western blot images show the protein expression of the several versions of Dun1 as well as the protein expression for the Rad53, Wtm1, and Crt1 ligands across samples. Protein expression of full-length Dun1 appears to be lower than that of Dun1 without the FHA domain and just the FHA domain, while ligand expression levels are the same throughout (Figure 3.3A-C).

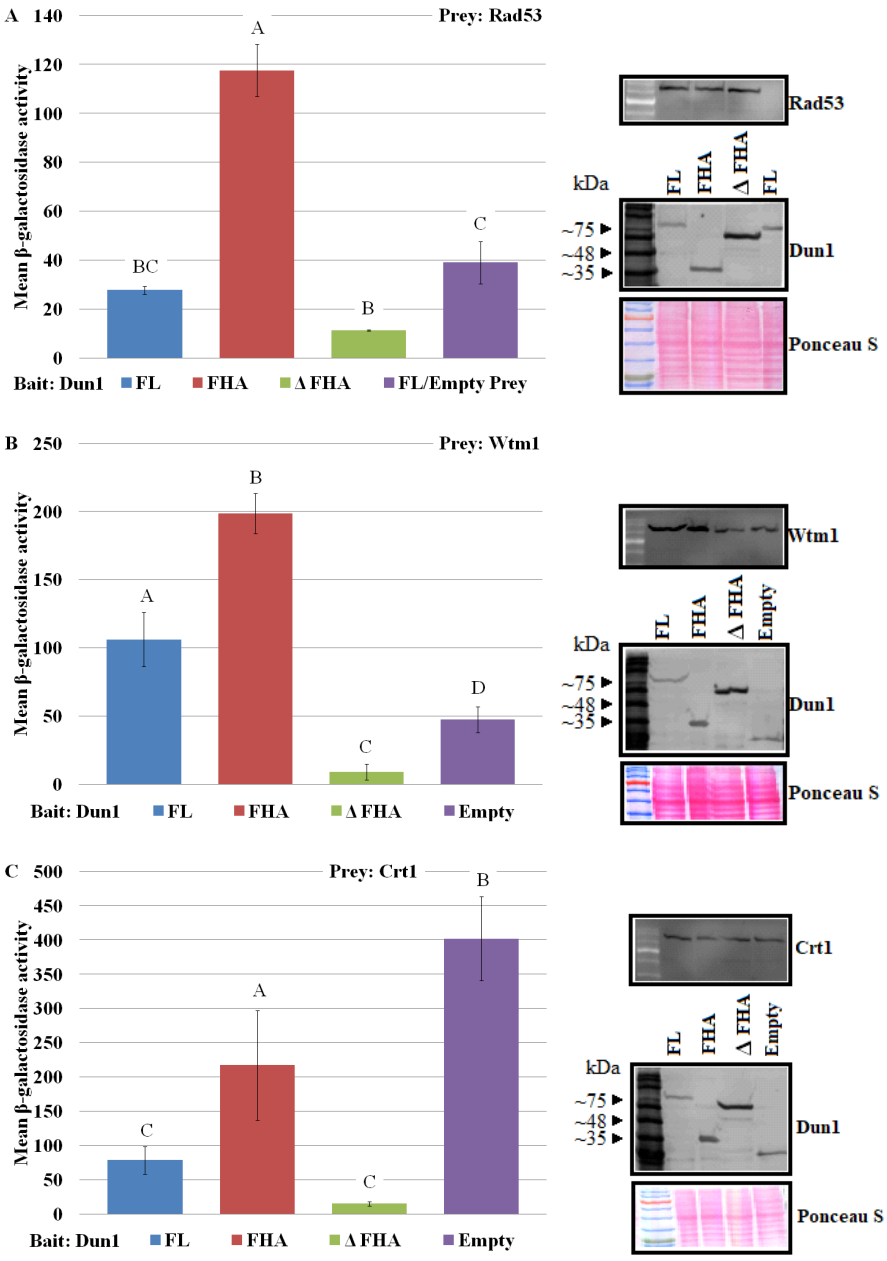

Figure 3.3: Analysis of the Interaction Between Dun1 and the Rad53, Wtm1, and Crt1 Ligands

Yeast two-hybrid assay analyses of the interactions between Dun1 and Rad53 (A), Dun1 and Wtm1 (B), and Dun1 and Crt1 (C). (A) Full-length Rad53 or an empty vector was the prey, with full-length (FL) Dun1, just the region of the Dun1 FHA domain (amino acids 21-145), or Dun1 without the FHA domain (Δ FHA) as the bait. (B) and (C) had Wtm1 and Crt1 as the prey, respectively, with Dun1 FL, Dun1 FHA, Dun1 Δ FHA, or an empty vector as the bait. Mean β-galactosidase activity units represent interaction strength, n = 3, and error bars represent standard deviation. Whole cell extracts were prepared following yeast two-hybrid assays in order to verify protein expression via western blot. Means with different letters are significantly different (Tukey's HSD, $p < 0.05$).

The previous assessment of the interaction between Dun1 FHA and Sml1 completed by an undergraduate student in the Duncker Lab (personal communication) revealed a systematic problem with the yeast two-hybrid assay where Sml1 in the pEG202 bait vector activates transcription of the *LacZ* reporter, independently of the prey construct's transcriptional activation domain, resulting in false positives. As a result, *SML1* was cloned into the pJG4-6 prey vector, effectively preventing the occurrence of the false positives, and yeast two-hybrid assays and corresponding western blots were used to evaluate Dun1 FHA domain necessity and sufficiency for the interaction with Sml1 (Figure 3.4A). Calculations of average β-galactosidase activity over three trials were graphed to depict the interaction strength between Dun1 and Sml1 (Figure 3.4A). Empty prey negative control levels of β-galactosidase activity were observed for the Dun1 FHA domain and Dun1 without the FHA domain with Sml1 while full-length Dun1 with Sml1 exhibited a high level of β-galactosidase activity (Figure 3.4A). This indicates that only full-length Dun1 that had both the FHA and kinase domains was able to interact with Sml1 (Figure 3.4A). Sequencing of Dun1 FHA domain prey constructs for FHA domain lateral surface interaction patch and pThr-binding site mutants used previously in the Duncker Lab for the evaluation of the Dun1 - Sml1 and Dun1 - Dif1 interactions revealed the absence of expected nucleotide substitutions that were supposed to change the key amino acid residues of the lateral surface interaction patch and the pThr-binding site. As a result, lateral surface interaction patch and pThr-binding site mutants were re-created and the Dun1 - Dif1 interaction was re-assessed after evaluating the necessity and sufficiency of the Dun1 FHA domain for the Dun1 - Dif1 interaction (Figure 3.4B - 3.6). Calculations of average β-galactosidase activity over three trials were graphed to depict the interaction strength between Dun1 and Dif1 (Figure 3.4B). Levels of β-galactosidase activity showed that a very strong interaction existed between full-length Dun1 that had both the FHA and kinase domains and Dif1 while a weakened interaction existed between Dif1 and just the FHA domain of Dun1 (Figure 3.4B). Without the FHA domain, there was no interaction between Dun1 and Dif1 (Figure 3.4B).

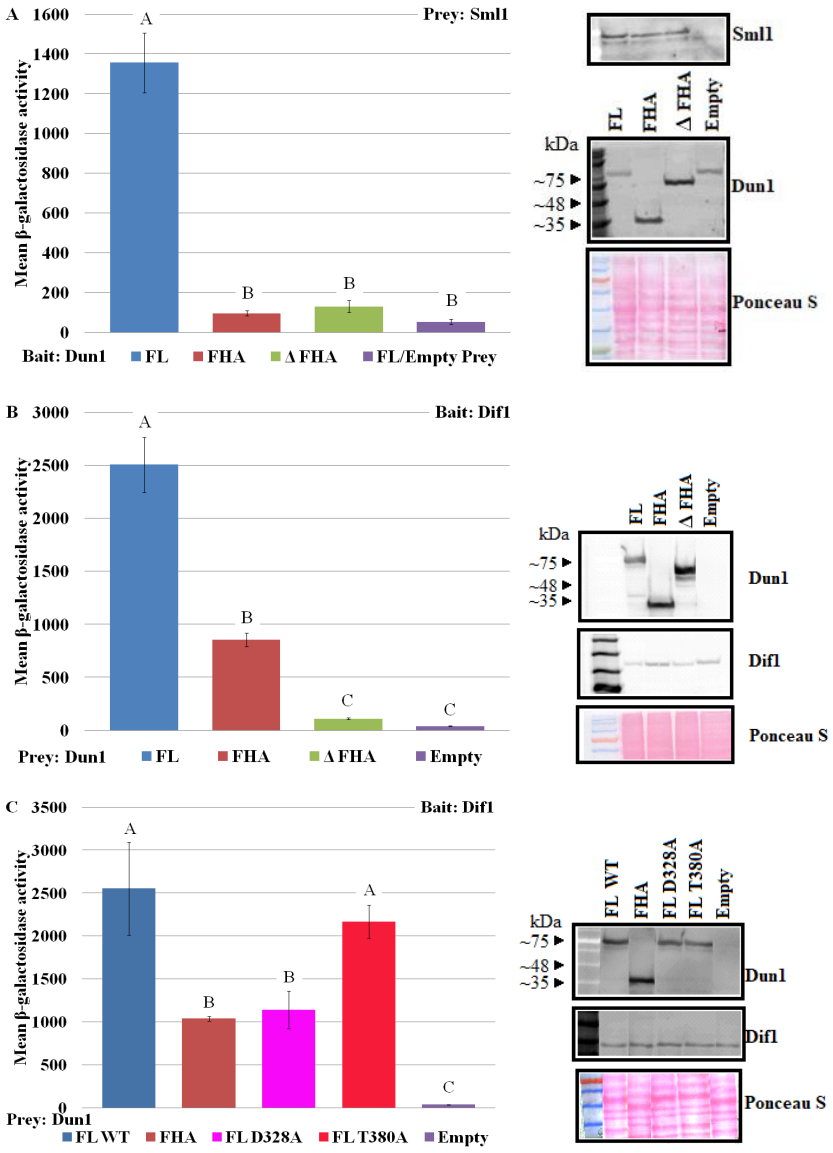

Figure 3.4: Analysis of the Interaction Between Dun1 and the Sml1 and Dif1 Ligands

Yeast two-hybrid assay analyses for the interaction between Dun1 and Sml1 (A) and Dun1 and Dif1 (B, C). (A) Full-length Sml1 or an empty vector was used as the prey with full-length (FL) Dun1, just the Dun1 FHA domain (amino acids 21-145), or Dun1 without the FHA domain (Δ FHA) as the bait. (B) Dun1 FL, Dun1 FHA, Dun1 without the FHA domain, or an empty vector was used as the prey with full-length Dif1 as the bait. (C) Dun1 FL, just the Dun1 FHA domain, mutants of the kinase domain within the context of full-length Dun1, or an empty vector was used as the prey with full-length Dif1 as the bait, in order to evaluate the contribution of the kinase domain to the Dun1 - Dif1 interaction. Mean β-galactosidase activity units represent interaction strength, n = 3, and error bars represent standard deviation. Whole cell extracts were prepared following yeast two-hybrid assays in order to verify protein expression via western blot. Means with different letters are significantly different (Tukey's HSD, $p < 0.05$).

The involvement of Dun1 kinase activity and/or Rad53-dependent Dun1 phosphorylation and activation in the Dun1 - Dif1 and Dun1 - Sml1 interactions was evaluated using yeast two-hybrid assays that included the following Dun1 kinase domain mutants: D328A, a substitution of the aspartic acid at position 328 to an alanine in order to eliminate Dun1 kinase activity from plasmid-expressed Dun1, and T380A, a substitution of the threonine at position 380 to an alanine preventing Rad53-dependent phosphorylation and activation of Dun1 (Zhou and Elledge, 1993; Zhao and Rothstein, 2002; Chen et al., 2007; reviewed in Sanvisens et al., 2014). Without the kinase domain, Dun1 was unable to interact with Sml1 (Figure 3.4A). However, absence of the kinase domain only weakened the interaction between Dun1 and Dif1 (Figure 3.4B). The 'kinase dead' D328A Dun1 mutant exhibited the same level of β-galactosidase activity when interacting with Dif1 as the Dun1 FHA domain while the T380A mutant of Dun1 that could not be phosphorylated and activated by Rad53 exhibited roughly the same level of β-galactosidase activity as full-length Dun1 when interacting with Dif1 (Figure 3.4C).

3.2.2 Highly conserved residues of the pThr-binding site and lateral surface interaction patch influence detectable genomic level protein expression

The 3-D ribbon diagrams corresponding to the surface models for the Dun1 FHA domain shown in Figure 3.2 are depicted in Figure 3.5. The ribbon diagrams show key residues that were selected for mutation of the canonical pThr-binding site and the candidate non-canonical FHA domain lateral surface interaction patch. Amino acid conservation colouring corresponds to Figure 3.2.

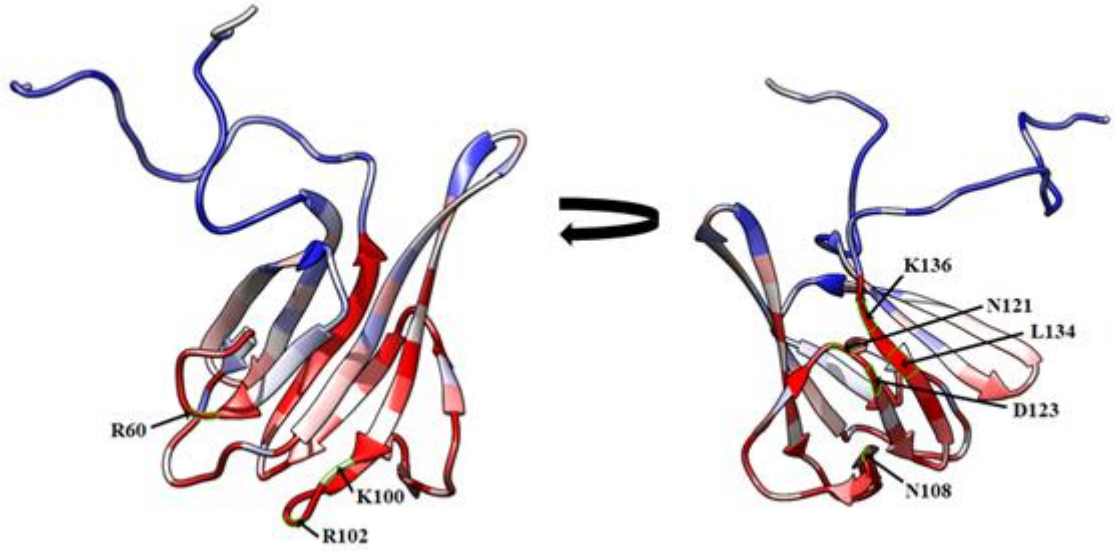

Figure 3.5: Conserved Surface Residues of the Dun1 FHA Domain Canonical pThr-binding Site and Non-canonical FHA Domain Lateral Surface Interaction Patch

Ribbon diagrams of the Dun1 FHA domain (PDB template ID: 2JQJ) showing candidate highly conserved residues selected for site-directed mutagenesis, using colours ranging from red (high conservation) to blue (low conservation), in order to evaluate the involvement of the pThr-binding site and/or lateral surface interaction patch of the Dun1 FHA domain in protein-protein interactions important for dNTP regulation. Letters refer to the single letter amino acid code with numbers representing amino acid position.

The Dun1 FHA domain has a di-phosphothreonine-binding motif at the pThr-binding site that is necessary for Dun1 recognition of hyperphosphorylated Rad53 (Lee et al., 2003; Lee et al., 2008b; Bashkirov et al., 2003; reviewed in Sanvisens et al., 2014). The arginine residue at position 60 (R60) is necessary for Dun1 FHA domain recognition of the first phosphothreonine residue in Rad53 while lysine

at position 100 (K100) and arginine at position 102 (R102) are both necessary for Dun1 FHA domain recognition of the second phosphothreonine in Rad53 (Lee et al., 2003; Lee et al., 2008b; Bashkirov et al., 2003; reviewed in Sanvisens et al., 2014). As a result, R60, K100, and R102 were selected to be changed into alanine (A) residues as mutants of the pThr-binding site of the Dun1 FHA domain. Amino acid residues of the lateral surface interaction patch selected for mutation were based on the criterion of being highly conserved surface residues. The following amino acids were previously selected in the Duncker Lab for lateral surface interaction patch mutants: asparagine 108 (N108), asparagine 121 (N121), aspartic acid 123 (D123), and lysine 136 (K136). Re-evaluation of the residues encompassed within the lateral surface patch revealed leucine 134 (L134) as another residue for mutation of the lateral surface interaction patch. The pThr-binding site mutants were designed as one single mutant, R60A, and one double mutant, K100A + R102A (KRA), for the mutation of the two arginines of the Dun1 FHA di-phosphothreonine recognition motif (Figure 3.5). Lateral surface interaction patch mutants featured amino acid substitutions from the wild-type residues to alanine and were initially designed as one double mutant, N108A + K136A (2M), and one quadruple mutant, N108A + N121A + D123A + K136A (4M) (Figure 3.5).

Graphs of the calculated average β-galactosidase activity over three trials illustrate the strength of the interaction between the Dun1 FHA domain and Dif1 for lateral surface interaction patch mutants (Figure 3.6A) and pThr-binding site mutants (Figure 3.6B). Both the 2M and 4M lateral surface interaction patch mutants of the Dun1 FHA domain exhibit the same levels of β-galactosidase activity as the empty bait negative control, indicating that mutations of the lateral surface interaction patch are able to completely abrogate the interaction between the Dun1 FHA domain and Dif1. The lack of change in the degree of interaction abrogation from the 2M to the 4M mutant implied that the N108A and K136A mutations of the 2M mutant were sufficient to completely disrupt the Dun1 FHA - Dif1 interaction. The R60A and KRA mutants of the pThr-binding site di-phosphothreonine recognition motif had the same levels of β-galactosidase activity as the empty bait negative control, showing the inability of Dun1 pThr-binding site mutants to interact with Dif1. Corresponding western blots show equal levels of protein

expression for the Dun1 mutants and Dif1, with the exception of the 2M and 4M Dun1 FHA domain mutants which appear to be lower than the WT Dun1 FHA domain level of protein expression.

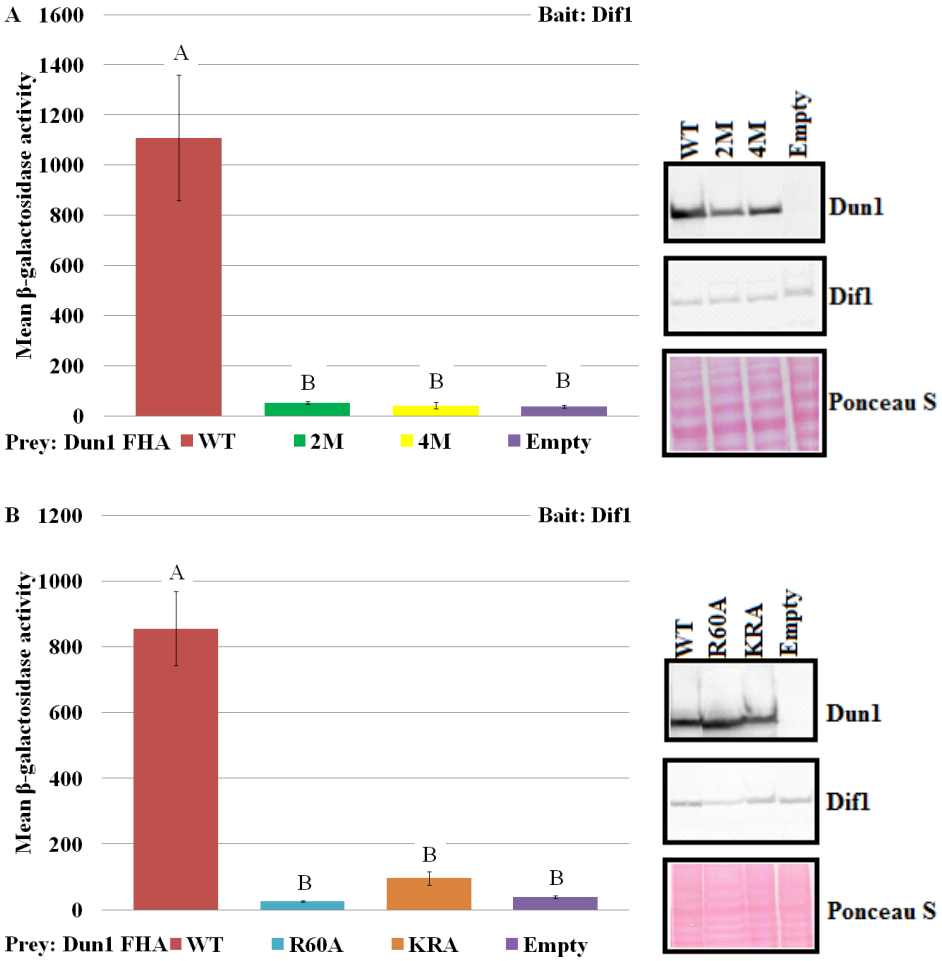

Figure 3.6: Analysis of the Interaction Between Dun1 FHA Domain Mutants and Dif1

Yeast two-hybrid assays evaluating the importance of the non-canonical FHA domain lateral surface interaction patch (A) and the canonical pThr-binding site (B) to the interaction between the Dun1 FHA domain and Dif1. Wild-type (WT) Dun1 FHA, mutants of the lateral surface interaction patch or pThr-binding site, or an empty vector was used as the prey with full-length Dif1 as the bait. Mean β-galactosidase activity units represent interaction strength, n = 3, and error bars represent standard deviation. Whole cell extracts were prepared following yeast two-hybrid assays in order to verify protein expression via western blot. (A) Point mutations changed asparagine 108, lysine 136, asparagine 121, and aspartic acid 123 to alanine. 2M and 4M denote a double and quadruple mutant of the non-canonical FHA domain lateral surface interaction patch of Dun1 [2M = N108A + K136A and 4M = N108A + K136A + N121A + D123A]. (B) Point mutations changed arginine 60, lysine 100 and arginine 102 to alanine. R60A and KRA denote a single and double mutant of the canonical pThr-binding site of Dun1 [KRA = K100A + R102A]. Means with different letters are significantly different (Tukey's HSD, $p < 0.05$).

Since the 2M mutations were enough to completely disrupt the interaction between the Dun1 FHA domain and Dif1, the mutations of the 2M mutant were split into an N108A single mutant and a K136A single mutant (Figure 3.7). The graph of average β-galactosidase activity calculated from three yeast two-hybrid trials shows that the N108A mutation of the lateral surface interaction patch reduces the Dun1 FHA domain - Dif1 interaction to roughly one-third of the strength of the interaction seen with the wild-type (WT) Dun1 FHA domain, a level similar to the empty vector negative control, which indicates complete disruption of the interaction (Figure 3.7A). The 2M double mutant and R60A single mutant both show a lack of interaction with Dif1 as seen in Figure 3.6A. The K136A single mutant exhibited an increase in the level of β-galactosidase activity relative to the WT Dun1 FHA domain for the interaction with Dif1, suggesting that the interaction between the Dun1 FHA domain and Dif1 is stronger with the K136A mutation of the lateral surface interaction patch (Figure 3.7B). The protein expression of Dun1 and Dif1 were confirmed via western blotting. Western blots show that the protein levels for the N108A and 2M Dun1 FHA mutants appear to be lower than that of the WT Dun1 FHA domain and the K136A mutant. The Dun1 2M FHA - Dif1 sample for Figure 3.7A was not expressing the Dif1 protein like the other samples.

Due to the unexpected increase in Dun1 FHA - Dif1 interaction strength for the Dun1 K136A FHA mutant, additional yeast two-hybrid assays were conducted to evaluate the extent of the increase in the interaction within the context of full-length Dun1 or in contrast to full-length WT Dun1 (Figure 3.8). Average β-galactosidase activity was calculated as a percentage of the WT for the analysis of the K136A mutation in full-length Dun1 over three trials (Figure 3.8A). The levels of β-galactosidase activity remain the same between the WT full-length Dun1 and K136A full-length Dun1 mutant with Dif1 (Figure 3.8A). The average β-galactosidase activity over three trials was graphed for the comparison of the K136A mutation in just the Dun1 FHA domain to full-length WT Dun1 and shows that the K136A mutation in the Dun1 FHA domain has a stronger interaction with Dif1 than full-length WT Dun1 (Figure 3.8B). The

corresponding western blots show relatively equal levels of protein expression with the exception of Dif1 in Figure 3.8A.

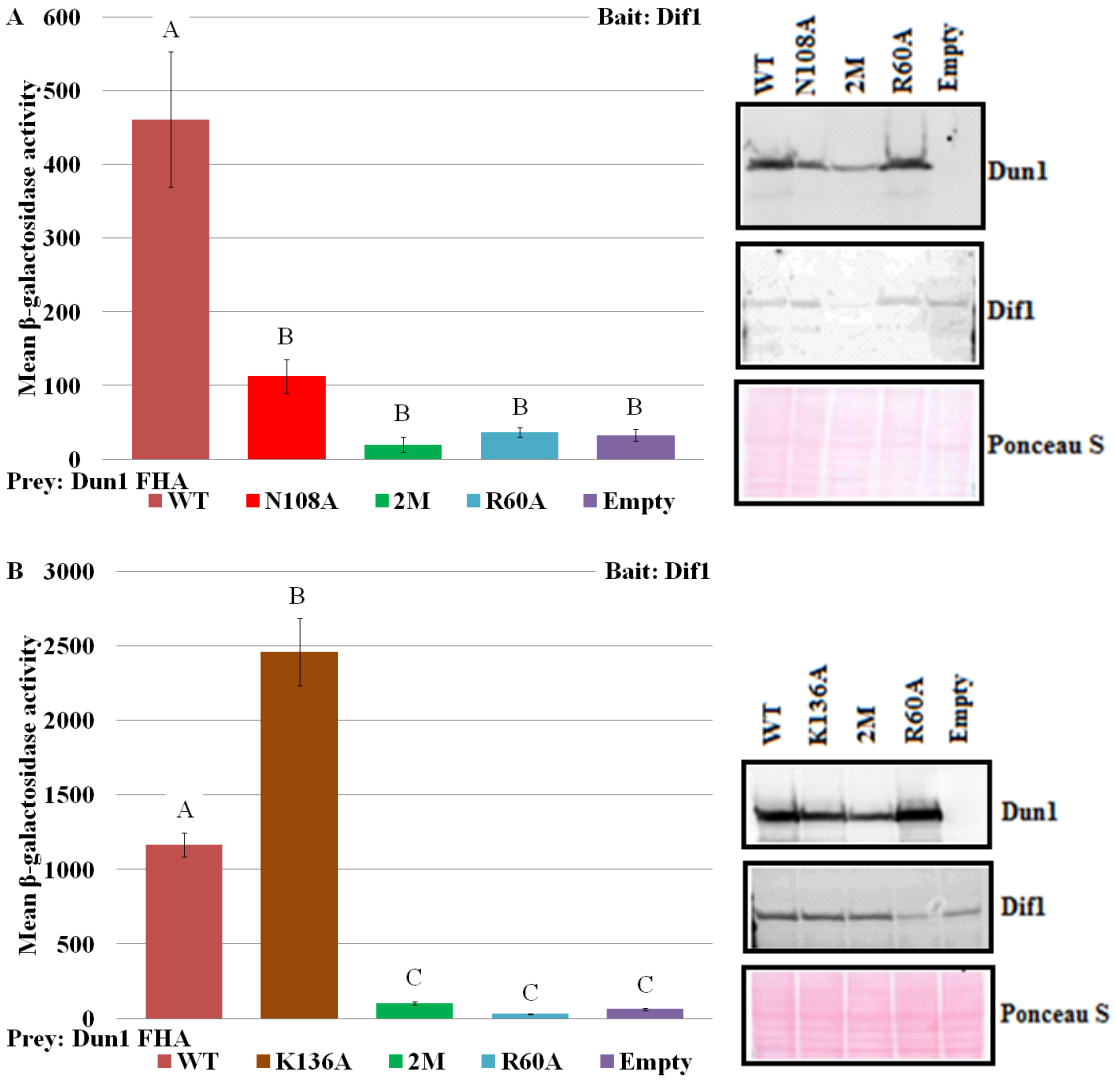

Figure 3.7: Dun1 FHA - Dif1 Interaction Analysis for the N108A and K136A Mutations

Yeast two-hybrid assays evaluating the effect of the (A) single N108A mutation, asparagine 108 converted to alanine, and the (B) single K136A mutation, lysine 136 converted to alanine, on the strength of the interaction between the Dun1 FHA domain and Dif1. Wild-type (WT) Dun1 FHA, single or double mutants of the non-canonical FHA domain lateral surface interaction patch, or an empty vector was used as the prey with full-length Dif1 as the bait [2M = N108A + K136A, a non-canonical FHA domain lateral surface interaction patch double mutant]. R60A is a single mutant of the canonical pThr-binding site where arginine 60 was changed to an alanine. Mean β-galactosidase activity units represent interaction strength, n = 3, and error bars represent standard deviation. Whole cell extracts were prepared following yeast two-hybrid assays in order to verify protein expression via western blot. Means with different letters are significantly different (Tukey's HSD, $p < 0.05$).

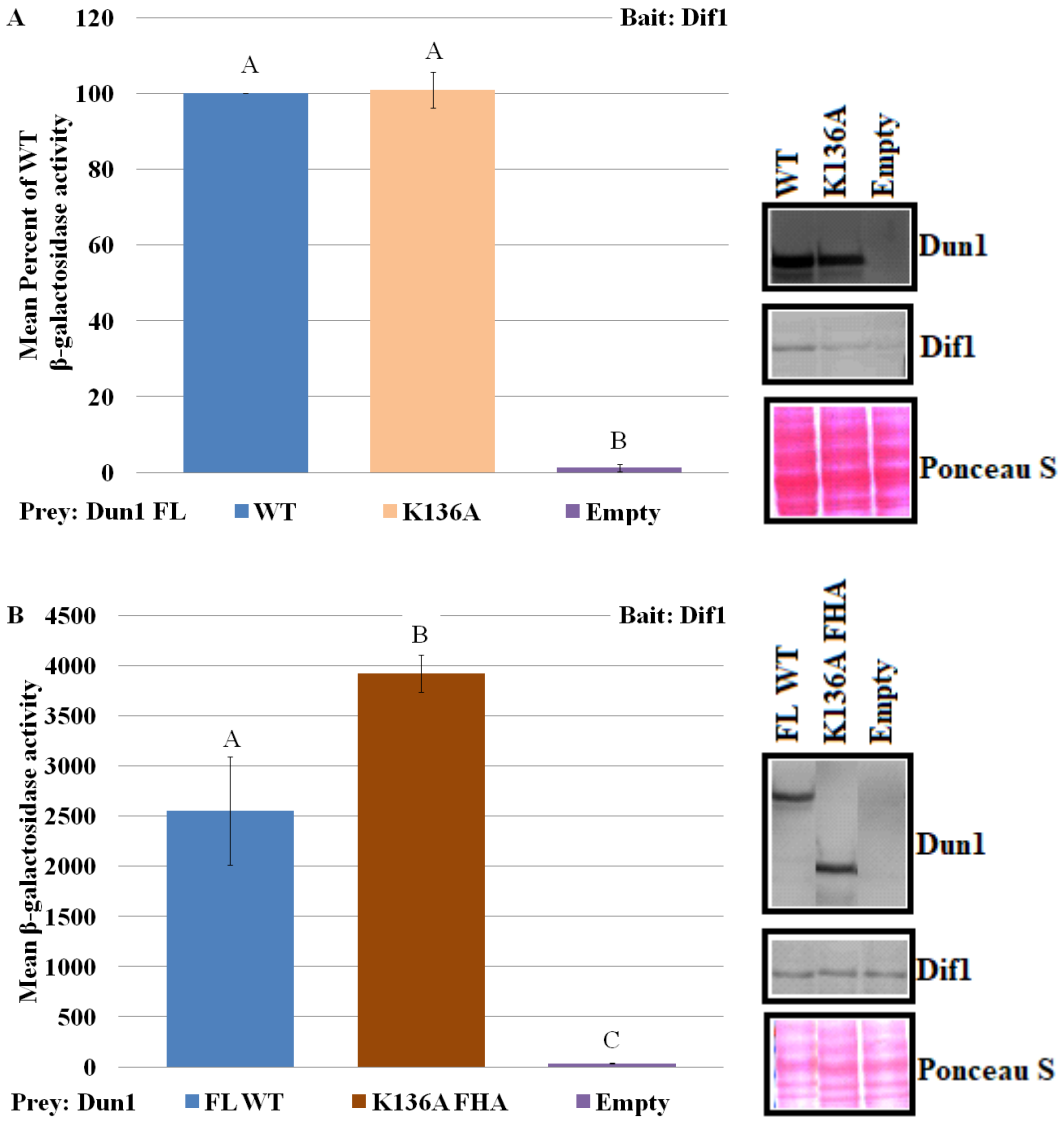

Figure 3.8: Analysis of the K136A Mutation in Full-length Dun1 and the Dun1 FHA Domain

Yeast two-hybrid assays evaluating the effect of the K136A, lysine 136 converted to alanine, mutation of the non-canonical FHA domain lateral surface interaction patch of the Dun1 FHA domain on its interaction with Dif1 in the context of full-length (FL) Dun1 (A) and just the FHA domain (B) compared to full-length wild-type (FL WT) Dun1. Wild-type full-length Dun1, mutant full-length Dun1, or an empty vector was used as the prey with full-length Dif1 as the bait (A) and wild-type full-length Dun1, mutant Dun1 FHA, or an empty vector was used as the prey with Dif1 as the bait (B). The mean percentage of the wild-type level of β-galactosidase activity units (A) and the mean β-galactosidase activity units (B) represent interaction strength, n = 3, and error bars represent standard deviation. Whole cell extracts were prepared following yeast two-hybrid assays in order to verify protein expression via western blot. Means with different letters are significantly different (Tukey's HSD, $p < 0.05$).

Spot plate assays were used to determine whether mutations of the pThr-binding site or lateral surface interaction patch would result in yeast cells being more or less sensitive to hydroxyurea, HU, or methyl methanesulfonate, MMS (Figure 3.9). The *dun1Δ* yeast strain was provided with full-length *DUN1* or *dun1* mutants harbouring a c-terminal myc13 tag, in order to monitor protein expression, from a yeast centromeric pRS315 plasmid which can mimic genomic expression due to the single copy number maintenance of the plasmid (Clarke and Carbon, 1980; Ishii et al., 2009; Stearns et al., 1990). Primary spot plate assays were used to assess the functional complementation of plasmid supplied Dun1. The spot plate assay shows that *dun1Δ* supplied with empty plasmid exhibits sensitivity to MMS and HU at a minimum of 0.015% MMS and 60 mM HU (Figure 3.9A). The addition of *DUN1* expressed from the pRS315 vector is able to rescue the sensitivity of the *dun1Δ* knock out mutant regardless of the addition of the c-terminal myc13 tag, confirming that not only is the pRS315 *DUN1* construct able to complement the *dun1Δ* genomic knockout, but that the addition of the c-myc13 tag for evaluating protein expression does not hinder Dun1 function. The 'untreated' control plate that does not have any genotoxic chemicals confirms the lack of any growth defects in the absence of genotoxic stress, indicating that any observed sensitivities on treated plates are a result of the genotoxic stress. The western blot confirms the addition of the c-myc13 tag and its usefulness in monitoring protein expression. Figure 3.9B shows the assessment of the genotoxic sensitivities of the *dun1Δ* yeast strain supplied with *DUN1* or *dun1* mutants, where the FHA domain has been mutated at the pThr-binding site or the lateral surface interaction patch, expressed from the pRS315 plasmid. The 'untreated' control plate again confirms that all samples initially grow successfully. At 80 mM HU all samples of *dun1Δ* supplied with plasmid-expressed *dun1* for lateral surface interaction patch mutations, with the exception of the R60A and K136A single mutations, begin to show sensitivity to HU; sensitivity can also be observed at 0.015% MMS. The *dun1Δ* samples with plasmid-expressed *dun1* for the R60A and K136A mutations exhibit slight but reproducible sensitivity to the highest concentrations of HU or MMS. The *dun1Δ* sample with plasmid-expressed *dun1* for the ΔFHA mutation shows sensitivity to HU, beginning at 80 mM, and to 0.015% MMS.

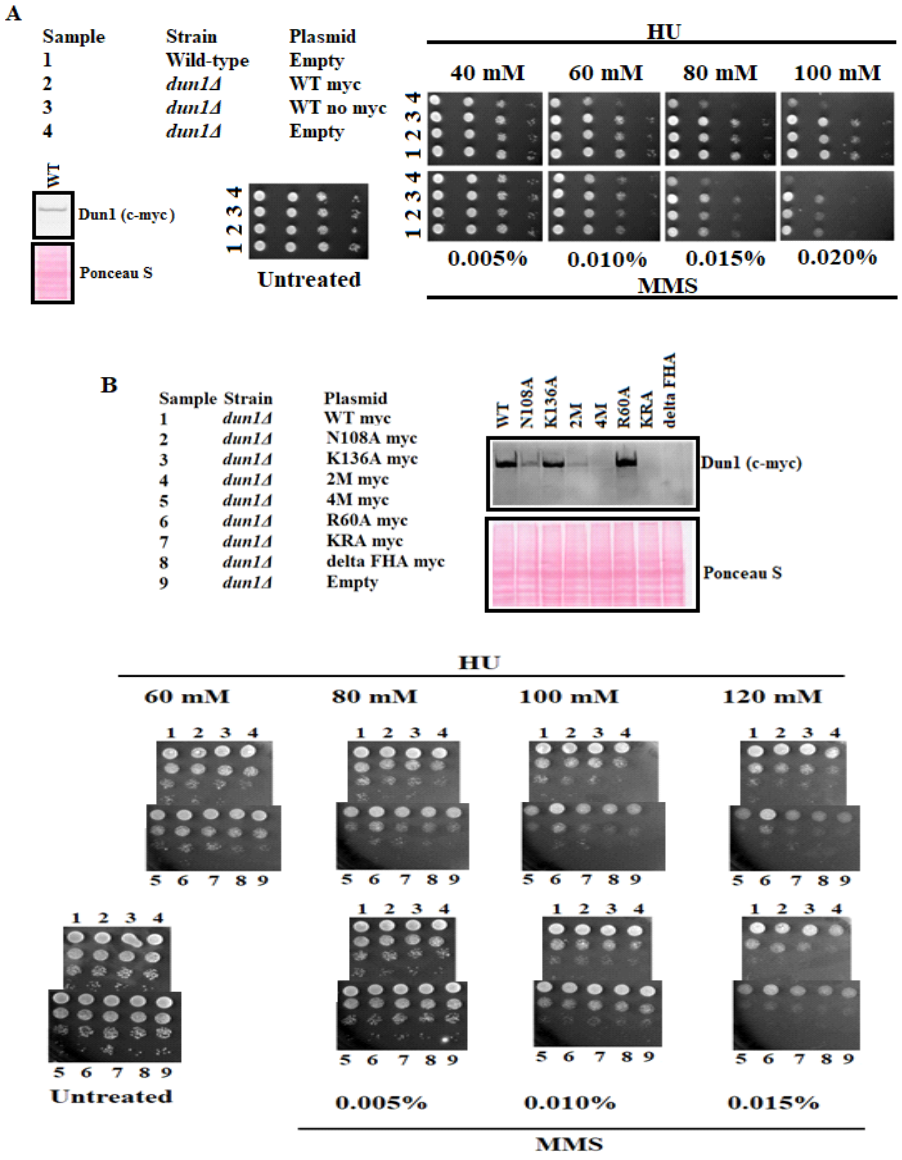

Figure 3.9: Functional Complementation of *dun1Δ* and Genotoxic Sensitivity Assessment for Dun1 FHA Mutants

Spot plate assays for (A) functional complementation of the *dun1Δ* genomic knockout with plasmid-expressed *c*-myc13-tagged Dun1 and (B) genotoxic sensitivity of yeast cells with plasmid-expressed *dun1* to hydroxyurea (HU) and methyl methanesulfonate (MMS). Whole cell extracts were prepared from cultures used for spot plate assays in order to verify protein expression via western blot. Plates were incubated for two days at 30°C. Mutants consisted of single, double, or quadruple mutations for select residues: asparagine 108, lysine 136, asparagine 121, aspartic acid 123, arginine 60, lysine 100, and arginine 102, changed to alanine or removal of the gene sequence for the FHA domain. Selective synthetic complete media lacking leucine was used for plasmid maintenance. Each row of samples represents one of four 10-fold serial dilutions spotted from the highest concentration of cells to the lowest.

The corresponding western blot shows that only the WT, K136A, and R60A versions of Dun1 are being expressed at the same level. The N108A mutant exhibits compromised protein expression, as does the 2M mutant, while the 4M, KRA and ΔFHA mutants are not visibly expressed.

Due to the slight genotoxic sensitivity observed for *dun1Δ* supplied with plasmid-expressed *dun1* for the K136A or R60A mutations, temperature and other genotoxic agents were included as independent variables for analysis (Figure 3.10). The Figure 3.9B spot plate assay was repeated, excluding the samples for mutants that did not show WT levels of protein expression, using incubation temperatures of either 30°C, the regularly used optimal temperature, or 37°C (Figure 3.10A). The increase in temperature, which can denature and destabilize proteins, coupled with HU or MMS stress was used in order to potentially amplify subtle growth defects. All samples collectively exhibited decreased growth on the plates incubated at 37°C compared to plates incubated at 30°C, but there was no effect on growth for the K136A or R60A mutant expressing samples compared to WT due to the increase in incubation temperature. The western blot confirmed equal expression of the WT, K136A, and R60A Dun1 proteins. Since an increased temperature coupled with HU or MMS exposure did not reveal an increase in the genotoxic sensitivity of the K136A or R60A mutant expressing samples, several other genotoxic chemicals used previously in the Duncker Lab: Bleomycin, Phleomycin, and Camptothecin, were selected for analysis in order to assess *dun1* mutant sensitivities to other types of genotoxic stress (Figure 3.10B). A preliminary spot plate assay was used to determine whether the *dun1Δ* genomic knockout strain was sensitive to Bleomycin, Phleomycin, or Camptothecin via the comparison of the *dun1Δ* strain to the highly sensitive *rad53Δsml1Δ* strain (Figure 3.10B). The lack of *dun1Δ* and *rad53Δsml1Δ* growth on the Bleomycin and Phleomycin plates relative to the untreated plate and their positive controls on treated plates demonstrates the observable sensitivity of the *dun1Δ* strain to Bleomycin and Phleomycin. The decrease in growth of *dun1Δ* and *rad53Δsml1Δ* on the Camptothecin plates relative to the untreated plate and their positive controls on treated plates demonstrates the observable sensitivity of the *dun1Δ* strain to Camptothecin. There was no requirement for the maintenance of an external plasmid for the initial

assessment of *dun1Δ* sensitivity to Bleomycin, Phleomycin, and Camptothecin shown in Figure 3.10B, so agar plates for that assay were made using YPD media instead of the selective SC drop out media used for all other spot plate assays where the pRS315 plasmid needed to be maintained. After the establishment of *dun1Δ* sensitivity to Bleomycin, Phleomycin and Camptothecin, the *dun1Δ* strain with plasmid-supplied *DUN1* or *dun1* mutants was tested for sensitivity to Bleomycin, Phleomycin, and Camptothecin using agar plates that were made with selective SC drop out media (data not shown). None of the samples grown on the selective SC plates showed any sensitivity to Bleomycin, Phleomycin, or Camptothecin. Most striking was the observation that even the *dun1Δ* strain supplied with an empty plasmid negative control did not show any sensitivity to Bleomycin, Phleomycin, or Camptothecin when it was already observed in Figure 3.10B that *dun1Δ* is sensitive to all three genotoxins. As a result, the spot plate assays were repeated using non-selective YPD media instead of selective SC drop out media (data not shown). The observations that the wild-type strain/empty plasmid sample exhibits growth on all YPD plates containing Bleomycin, Phleomycin, or Camptothecin while the *dun1Δ* strain/empty plasmid sample has compromised growth on YPD plates containing Bleomycin, Phleomycin, or Camptothecin indicate that the type of media may influence the activity of Bleomycin, Phleomycin, and Camptothecin. As a result, the analysis of *dun1Δ* with plasmid-supplied *DUN1* or *dun1* mutants remains inconclusive due to the lack of selective pressure for plasmid maintenance with YPD media.

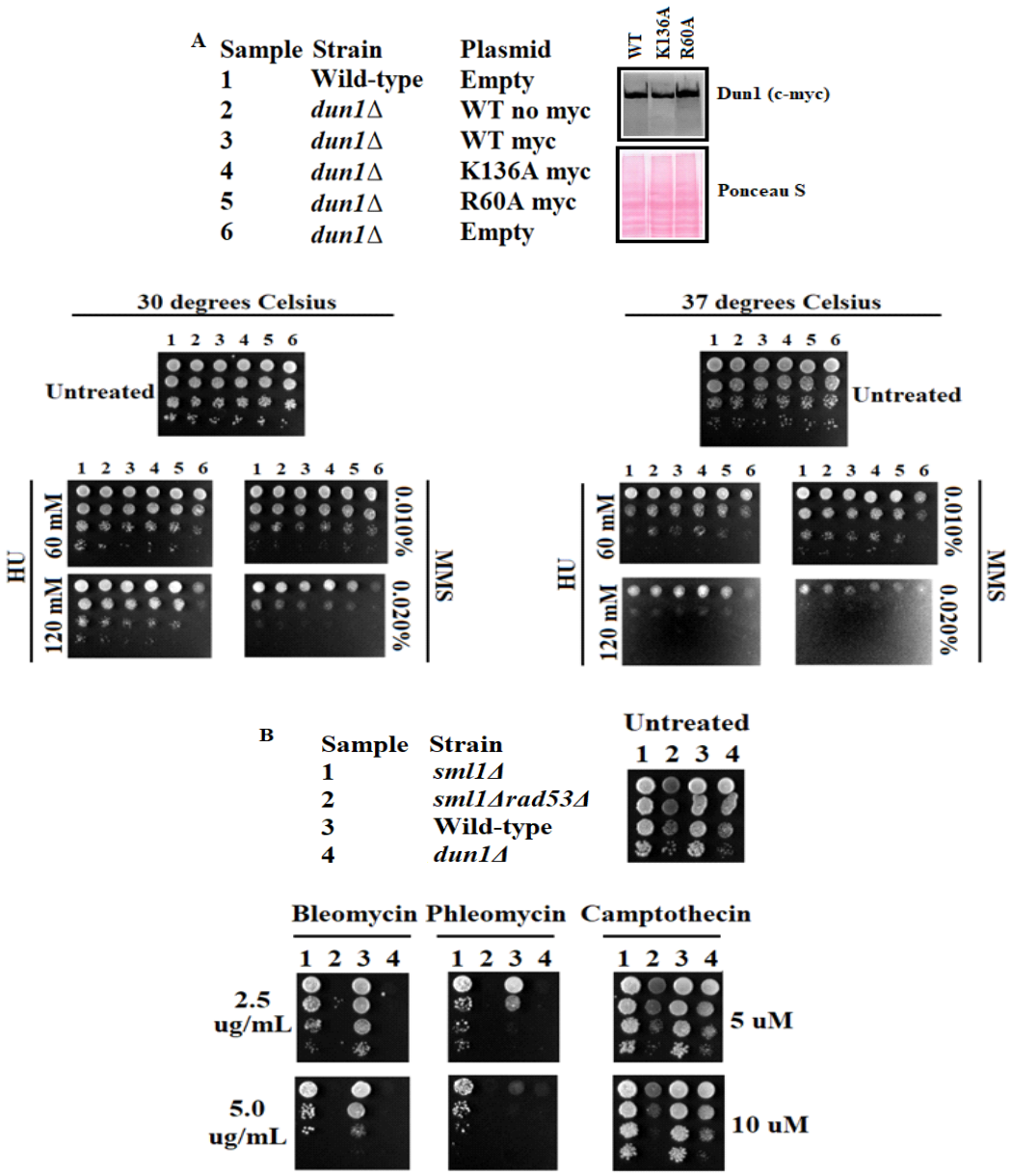

Figure 3.10: Assessment of Genotoxic Sensitivity with Increased Temperature or Other Genotoxins

Spot plate assays evaluating sensitivity of wild-type (has genomic copy of *DUN1*) or *dun1Δ* (genomic knockout of *DUN1)* yeast strains supplied with an empty plasmid or a plasmid construct expressing wild-type (WT) *DUN1* or mutant *dun1* with WT-level protein expression to (A) hydroxyurea (HU) or methyl methanesulfonate (MMS) at 30°C or 37°C. (B) Control spot plate assay comparing the expected sensitivity of the *sml1Δrad53Δ* yeast strain to its *RAD53* counterpart, *sml1Δ,* and the *dun1Δ* strain and its corresponding wild-type strain. Solid agar growth media was YPD without selection (B). The myc tag allows for the evaluation of Dun1 expression via western blotting. Plates were incubated for two days at 30°C. Plates shown in panel A were incubated at 37°C for two days. Each row of samples represents one of four 10-fold serial dilutions spotted from the highest concentration of cells to the lowest.

3.2.3 K136-central projection of the Dun1 non-canonical FHA domain lateral surface interaction patch contributes to interactions involved in dNTP regulation

The re-assessment of the ribbon diagram showing highly conserved lateral surface interaction patch residues revealed a side-chain 'projection' on the lateral surface of the Dun1 FHA domain (Figure 3.11). The largest contribution to this projection came from the side-chain of lysine 136. In addition to lysine 136, the asparagine 121 (N121) and leucine 134 (L134) side-chains also contribute to this surface projection. Due to the observation that the K136A Dun1 single mutant had a WT Dun1 level of protein expression from the pRS315 plasmid, N121A and L134A were created as two Dun1 lateral surface interaction patch single mutants to be included in yeast two-hybrid assays (Figure 3.12), evaluated for stable protein expression, and then used to assess HU and MMS sensitivity (Figure 3.13).

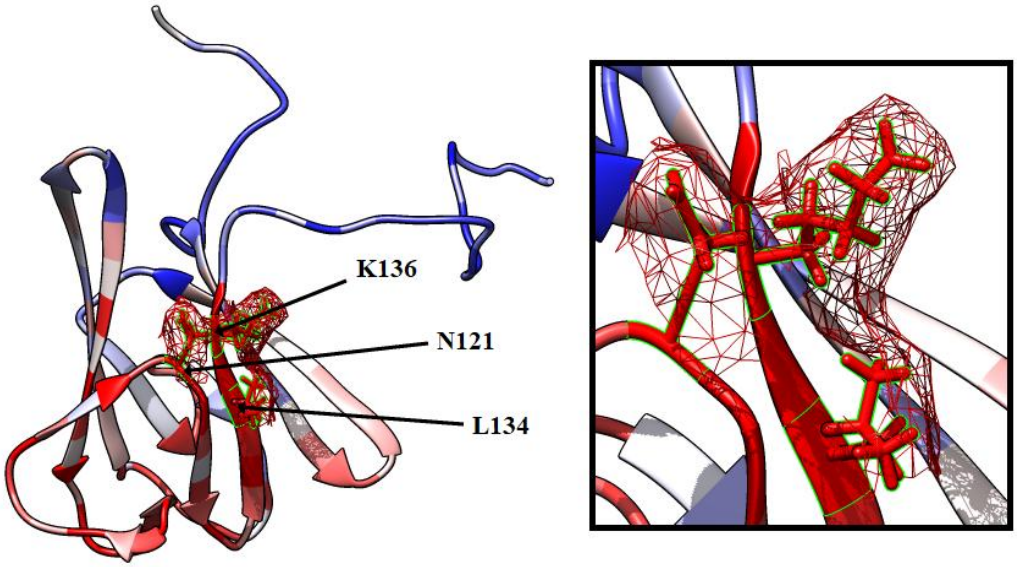

Figure 3.11: Illustration of the K136-central Projection on the Dun1 FHA Domain Lateral Surface Interaction Patch

Ribbon diagram of the 3-D model for the Dun1 FHA domain (PDB template ID: 2JQJ) showing conservation of FHA domain residues with colours ranging from red (high conservation) to blue (low conservation) and depicting the side-chain projections of the lysine 136 (K136) amino acid and two neighbouring residues asparagine 121 (N121) and leucine 134 (L134). Side chains were coloured according to the conservation level of their associated residue with a mesh outline illustrating the surface of the residue.

The N121A and L134A single mutants were added as potential lateral surface interaction patch mutants that could disrupt the interactions between the Dun1 FHA domain and Dif1 or Sml1. Yeast two-hybrid assays were used to evaluate whether the N121A and L134A single mutants had any effect on the interactions of Dun1 with Dif1 (Figure 3.12A) or Sml1 (Figure 3.12B). Calculations of the average β-galactosidase activity over three trials were graphed to illustrate that neither the N121A mutation nor the L134A mutation have any effect on the interaction strength between the Dun1 FHA domain and Dif1 (Figure 3.12A). As observed previously, the K136A mutation generated a large increase in the interaction strength between the Dun1 FHA domain and Dif1 while the R60A mutation completely abrogated the interaction. The corresponding western blot shows equal levels of Dun1 and Dif1 expression across samples. The graph shown in Figure 3.12B shows the calculated averages of β-galactosidase activity over three trials for the assessment of the Dun1 - Sml1 interaction. The N121A mutation has no affect on the interaction between full-length Dun1 and Sml1 whereas the L134A mutation reduces the interaction strength by approximately 50% (Figure 3.12B). In contrast to the Dun1 - Dif1 interaction, the K136A mutation decreases the strength of the Dun1 - Sml1 interaction by approximately one-third, while the R60A mutation reduces the interaction strength to less than half of the WT Dun1 - Sml1 interaction. The corresponding western blot shows that both Dun1 and Sml1 exhibit equivalent levels of protein expression across samples.

The R60A, N121A, L134A, and K136A Dun1 single mutants were then expressed for spot plate assay assessments of HU and MMS genotoxic sensitivity in the *dun1Δ* yeast strain (Figure 3.13). Samples of *dun1Δ* supplied with plasmid-expressed *dun1* for the K136A or R60A mutations continued to only show slight but reproducible sensitivity to the highest concentrations of HU or MMS relative to the wild-type/empty plasmid positive control sample, while *dun1Δ* supplied with plasmid-expressed *dun1* for the N121A or L134A mutations exhibited stronger sensitivity to HU at 150 mM and MMS at 0.015%, although still not as much as the *dun1Δ*/empty plasmid negative control sample. The western blot

confirmed equivalent levels of protein expression for all Dun1 mutant proteins relative to WT Dun1 (Figure 3.13).

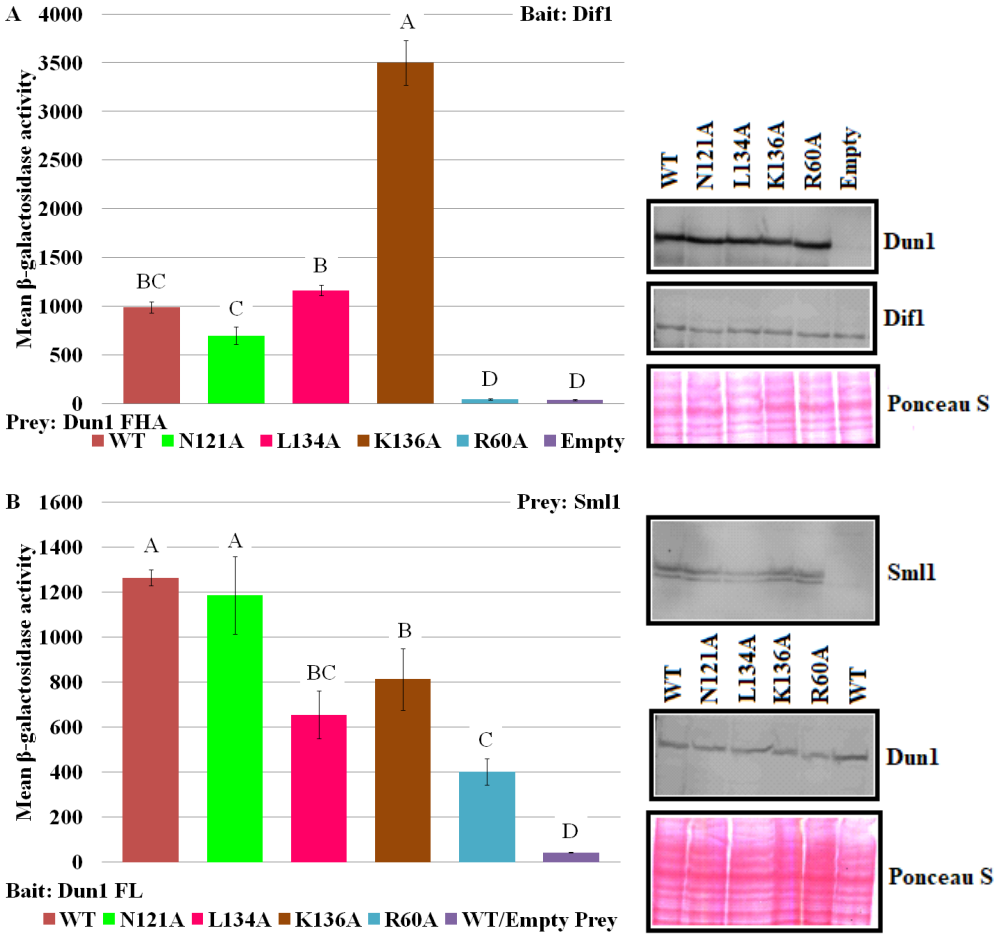

Figure 3.12: Analysis of the K136-central Projection Substitution Mutants for the Dun1 - Dif1 and Dun1 - Sml1 Interactions

Yeast two-hybrid assays evaluating the change in interaction strength between Dun1 and Dif1 (A) or Sml1 (B) with a variety of Dun1 FHA domain mutants. (A) Wild-type (WT) Dun1 FHA, indicated mutants of the FHA domain, or an empty vector was used as the prey with full-length Dif1 as the bait. (B) Full-length Sml1 or an empty vector was used as the prey with WT full-length (FL) Dun1 or indicated Dun1 FL mutants as the bait. Missense mutations were used to change the highly conserved asparagine 121 (N121), leucine 134 (L134), lysine 136 (K136), and arginine 60 (R60) residues into alanine in order to mutate the non-canonical FHA domain lateral surface interaction patch (N121A, L134A, and K136A) or the canonical pThr-binding site (R60A). Mean β-galactosidase activity units represent interaction strength, n = 3, and error bars represent standard deviation. Whole cell extracts were prepared following yeast two-hybrid assays in order to verify protein expression via western blot. Means with different letters are significantly different (Tukey's HSD, $p < 0.05$).

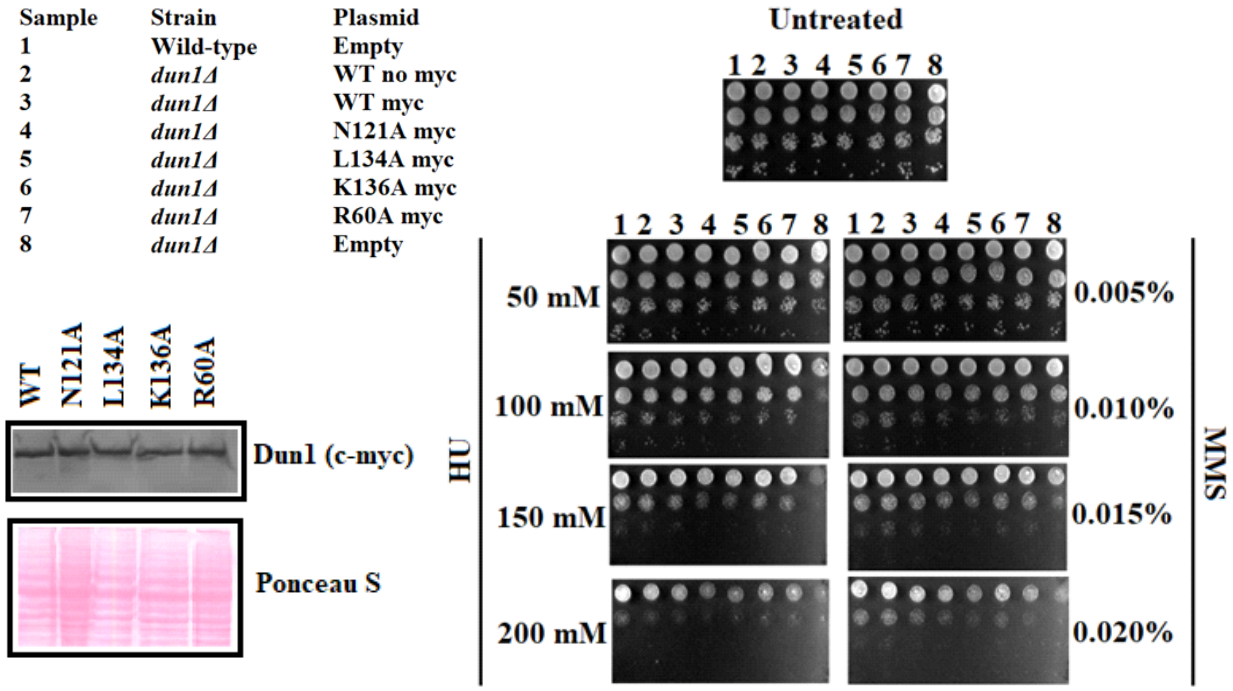

Figure 3.13: Genotoxic Sensitivity Analysis for K136-central Projection Mutants

Spot plate assay evaluating the sensitivity of wild-type (has genomic copy of *DUN1*) or *dun1Δ* (genomic knockout of *DUN1)* yeast strains supplied with an empty plasmid or a plasmid construct of wild-type (WT) *DUN1* or mutant *dun1* with WT Dun1 levels of protein expression (verified via western blot using the c-myc tag added to the c-terminus of the Dun1 coding sequence in the pRS315 plasmid) to hydroxyurea (HU) or methyl methanesulfonate (MMS). Solid agar growth media was synthetic complete (SC) media lacking leucine, for selection. All plates were incubated for two days at 30°C. Mutants consisted of single missense mutations of the non-canonical FHA domain lateral surface interaction patch (N121A, L134A, and K136A) and the canonical pThr-binding site (R60A). Highly conserved asparagine 121 (N121), leucine 134 (L134), lysine 136 (K136), and arginine 60 (R60) were changed to alanine. Each row of samples represents one of four 10-fold serial dilutions spotted from the highest concentration of cells to the lowest.

3.3 Discussion

The data described throughout this thesis both confirms the existence of the conserved non-canonical FHA domain lateral surface interaction patch on the Dun1 FHA domains and illuminates its contribution to protein-protein interactions involved in dNTP regulation. The yeast two-hybrid assays shown in Figures 3.3 and 3.4 demonstrate the importance of the Dun1 FHA domain to Dun1-based protein-protein interactions. Unique to the interaction between Dun1 and Sml1, both the FHA and kinase

domains were necessary for the interaction (Figure 3.4A). For the Dun1 - Dif1 interaction, the FHA domain was necessary for the interaction but not fully sufficient (Figure 3.4B). Removal of the Dun1 kinase domain weakened the Dun1 - Dif1 interaction and the disruption of the kinase activity of plasmid-expressed Dun1 weakened the Dun1 - Dif1 interaction to the same extent as removal of the kinase domain, suggesting that Dun1 phosphorylation may contribute to protein-protein interactions between Dun1 and its downstream ligands (Figure 3.4C). The FHA domain of Dun1 on its own was sufficient for interaction with the Rad53, Wtm1, and Crt1 ligands (Figure 3.3). Since most of the Dun1 ligands exhibit prior associations with other proteins as part of their regular inhibitory functions, it may be that the interactions between Dun1 and its ligands are based on competitive binding (Lee and Elledge, 2006; Lee et al., 2008a; Andreson et al., 2010; reviewed in Tsaponina et al., 2011 and Sanvisens et al., 2016). The low β-galactosidase activity levels for the interactions between Dun1 without its FHA domain and the Rad53, Wtm1, and Crt1 ligands relative to the empty vector negative control and/or other samples that indicated a lack of detectable protein-protein interactions was unexpected. The current speculation remains that removal of the entire FHA domain results in the decreased opportunity for chance occurrences of bait and prey construct proximity as it was anticipated that their β-galactosidase activity levels would be the same as the empty vector negative controls and other samples without observable interactions.

The reduction or lack of protein expression for the N108A, 2M, 4M, Δ FHA, and KRA Dun1 mutants for the spot plate assay shown in Figure 3.9B demonstrated that the decrease in β-galactosidase activity observed between the Dun1 N108A FHA mutant and Dif1 was likely not a result of interaction abrogation but rather due to a decrease in Dun1 protein levels for the Dun1 N108A mutant (Figure 3.7A) and that the interaction abrogation observed for the 2M, 4M, and KRA mutants were also likely due to diminished protein expression (Figure 3.6). The same cannot be said of the Dun1 Δ FHA mutant seen throughout Figures 3.3 and 3.4 because there was not an obvious decrease in the over-expression of the Dun1 Δ FHA mutant protein like there was for the N108A, 2M, 4M, and KRA mutants during the yeast

two-hybrid assays. While the K136A and R60A Dun1 mutants did show WT levels of protein expression in Figure 3.9B, there was only slight but reproducible sensitivity of *dun1Δ* expressing those mutant versions of *dun1* to the highest concentrations of HU or MMS (Figure 3.9B, 3.10A). Despite the fact that little to no sequence homology exists amongst the vast collection of discovered FHA domains, the structure is highly conserved (reviewed in Mahajan et al., 2008). The observation that mutating highly conserved residues located within the lateral surface interaction patch and pThr-binding site caused compromised protein expression, suggests that highly conserved residues within the lateral surface interaction patch as well as the pThr-binding site may contribute to protein stability as well as the establishment of protein-protein interactions.

The spot plate assays testing Bleomycin, Phleomycin, and Camptothecin sensitivity yielded an unexpected result (data not shown). Whereas HU and MMS are able to cause genotoxic sensitivity to *dun1Δ* on SC media lacking leucine, leucine drop out provides the selective pressure that ensures the maintenance of the pRS315 plasmid, neither Bleomycin, Phleomycin, nor Camptothecin appear to function on SC media lacking leucine (data not shown). As a result, no conclusions could be made about the genotoxic sensitivity of *dun1Δ* expressing mutant versions of *dun1*. In order to properly assess the effects of those genotoxins, the mutations of interest will need to be created within the genome as opposed to being expressed from an external plasmid thereby removing the need to use selective drop out media.

The most fruitful analyses were generated after the discovery of the K136-central projection on the lateral surface interaction patch (Figure 3.11). The addition of the N121A and L134A Dun1 single mutants to the collection of mutants included in the yeast two-hybrid assays (shown in Figure 3.12) revealed a contrasting pattern to the interaction between Dun1 and Dif1 compared to Dun1 and Sml1, a revelation that might help explain the slight HU and MMS sensitivity seen with *dun1Δ* samples expressing the K136A and R60A *dun1* mutants from the pRS315 plasmid shown in Figure 3.9B and 3.10A. For the Dun1 - Dif1 interaction, neither the N121A mutation nor the L134A mutation had any

effect (Figure 3.12A). The K136A mutation generated a huge increase in the strength of the interaction while the R60A mutation completely disrupted the interaction (Figure 3.12A). The pattern is mostly reversed for the Dun1 - Sml1 interaction (Figure 3.12B). The N121A mutation exhibited no effect on the interaction strength between Dun1 and Sml1 whereas the L134A mutation decreased the strength of the interaction (Figure 3.12B). The K136A mutation also reduced the interaction strength and, unlike the Dun1 - Dif1 interaction, the R60A mutation reduced the interaction strength as opposed to completely disrupting it, suggesting that both the pThr-binding site and the lateral surface interaction patch are needed for the Dun1 - Sml1 interaction. The pThr-binding site appears to be the primary interface for the Dun1 - Dif1 interaction with the lateral surface interaction patch functioning only to modulate the strength of the interaction and/or the initial affinity between Dun1 and Dif1 (Figure 3.12B).

The Figure 3.13 spot plate assay shows that the N121A and L134A-expressing *dun1Δ* mutants show sensitivity to HU and MMS while the K136A and R60A-expressing *dun1Δ* mutants only showed slight sensitivity to the highest concentrations of HU and MMS. The slight sensitivity of the latter two samples was initially surprising when it was observed in Figure 3.9B and again in Figure 3.10A, but considering the pattern with which Dun1 interacts with Dif1 and Sml1, the lack of sensitivity may just be a reflection of the complexity and/or multi-faceted nature of the Dun1 contribution to dNTP regulation keeping in mind that the effects of the mutations have only been analyzed for the Dif1 and Sml1 ligands so far. The K136A mutation exhibits no detrimental effect to the Dun1 - Dif1 interaction when in the context of full-length Dun1, although it increases the interaction strength between the Dun1 FHA domain and Dif1 beyond the level of the Dun1 FL - Dif1 interaction when in the context of just the FHA domain, likely due to the isolation of the FHA domain and the change in the size of the side chain as a result of the mutation (Figure 3.8). With respect to the Dun1 - Sml1 interaction, the K136A mutation only weakens the strength of the interaction and not by more than 50% (Figure 3.12B). Considering dNTP regulation as a whole, the K136A mutation alone would not likely have a very drastic defect on the ability of a cell to still manage to regulate dNTP levels especially given the fact that there are multiple factors involved in

regulating dNTP synthesis. On the other hand, the R60A mutation completely disrupted the Dun1 - Dif1 interaction and weakened the Dun1 - Sml1 interaction but still did not show strong HU and MMS sensitivity (Figure 3.12-3.13). One could speculate that the lack of strong sensitivity may be because the R60A mutant is still able to interact with other Dun1 ligands, at least marginally, in order to relieve enough of the collective inhibitory activities involved in dNTP regulation to still permit adequate dNTP synthesis when cells are stressed, but confirmation would depend on an evaluation of the effects of the R60A mutant on the other Dun1 interactions keeping in mind that the Dun1 FHA pThr-binding site has a di-phosphothreonine-recognition motif, although it has currently only been shown to contribute to the Rad53 - Dun1 interaction (Lee et al., 2003; Lee et al., 2008b; Bashkirov et al., 2003; reviewed in Sanvisens et al., 2014). The observations that the N121A and L134A mutations generate, to a degree, genotoxic sensitivity suggests that some mutations may disrupt more interactions than others and that by doing so are more capable of interfering with dNTP regulation.

Chapter 4

General Conclusions and Future Directions

4.1 The Dun1 kinase domain and the non-canonical FHA domain lateral surface interaction patch influence protein-protein interactions involved in dNTP regulation

The initial yeast two-hybrid assays confirming the existence of protein-protein interactions between Dun1 and the other proteins involved in the dNTP regulation pathway demonstrated the importance of the Dun1 FHA domain to those interactions. Establishment of the interactions between Dun1 and two of its ligands, Dif1 and Sml1 depended on both the Dun1 FHA and kinase domains, while only the Dun1 FHA domain seemed to be able to interact with the Rad53, Wtm1, and Crt1 ligands. The unexpected observation that Crt1 could activate β-galactosidase activity on its own in the two-hybrid assay was likely due to an interaction between Crt1 in the prey vector and the LexA operators on the reporter vector in the absence of Dun1 as the bait. This implicated Dun1 as being a protein that utilizes competitive binding, an implication supported by the fact that Dun1 is not the 'customary' binding partner for other proteins involved in dNTP regulation as Wtm1, Crt1, Dif1, and Sml1 all carry out their normal inhibitory functions via their associations with other proteins.

Yeast two-hybrid assays evaluating the Dun1 FHA domain mutants with respect to the Dun1-Dif1 and Dun1-Sml1 interactions proved that the identified patch of conserved residues on the lateral surface of the Dun1 FHA domain constitute a non-canonical FHA domain lateral surface interaction patch that contributes to Dun1 protein-protein interactions both independently and in conjunction with the canonical pThr-binding site. The collection of Dun1 mutants that were examined revealed that highly conserved residues of the lateral surface interaction patch and the pThr-binding site participate in FHA

domain-based protein-protein interactions and that mutations of some conserved residues compromise 'genomic level' protein expression.

The multiple downstream targets of Dun1 each carry out individual yet interconnected functions. Single mutants of the Dun1 FHA domain had different effects on the strength of the interactions between Dun1 and its downstream targets. Spot plate assays examining Dun1 mutants showed that only some cases of *dun1Δ* strain transformants expressing mutant *dun1* from the pRS315 plasmid exhibited sensitivity to HU and MMS. The observed instances of genotoxic sensitivity and the strength of the sensitivity did not necessarily correspond with Dun1 FHA mutants that were able to disrupt Dun1 interactions, suggesting that the complexity of the dNTP regulation pathway allows cells to cope with the loss of single parts of the pathway. Together the results of the yeast two-hybrid and spot plate assays proved the involvement of the lateral surface interaction patch in the protein-protein interactions orchestrating dNTP regulation and their importance to genotoxic stress resistance.

4.2 Future Directions

The data presented in this thesis presents an excellent general examination of the dNTP regulation pathway and the Dun1 FHA domain-based protein-protein interactions that orchestrate it. The results also demonstrate the value of investigating other FHA domain-containing proteins in budding yeast and looking for the existence of additional conserved FHA domain lateral surface interaction patches. However, in order to establish an understanding of Dun1 ligand recognition and binding as well as the Dun1 FHA domain lateral surface interaction patch and its contribution to dNTP regulation that is both cohesive and comprehensive, all remaining ambiguities need to be addressed. Upon discovering that the kinase domain, the only other structured region of Dun1, was necessary for the Dun1-Sml1 interaction, the contribution of the kinase domain was evaluated with respect to the Dun1-Dif1 interaction. D328A and T380A kinase domain single mutants were incorporated into yeast two-hybrid assays evaluating the interaction between Dun1 and Dif1 showing that the kinase activity of plasmid-expressed Dun1

contributed to the full-length Dun1 interaction with Dif1. The same mutants should be tested with Sml1 in order to determine whether the Dun1-Sml1 interaction benefits from the kinase domain in a similar fashion.

Protein-protein interactions were observed between the Dun1 FHA domain and the Rad53, Wtm1, and Crt1 ligands, but the effects of Dun1 FHA mutations on those interactions have yet to be tested. In order to make any strong conclusions about the frequency of disrupted protein-protein interactions due to a particular mutation, all interactions need to be assessed. As such, yeast two-hybrid assays should be used to examine whether the lateral surface interaction patch and pThr-binding site mutants have any effect on the interactions between the Dun1 FHA domain and the Rad53, Wtm1, or Crt1 ligands. A modification of the typical yeast two-hybrid assay that introduces another vector containing the coding sequence for a protein that could compete with Dun1 for interactions with Rad53, Wtm1, or Crt1 could be used to examine whether Dun1-based interactions rely on competitive binding to induce dNTP synthesis. Mass spectroscopy and/or Nuclear Magnetic Resonance (NMR) of purified full-length Dun1 or just the region of the Dun1 FHA domain could be used to determine the existence of any post-translational modifications to the Dun1 FHA domain at or around the position of lysine 136 that might explain the increase in Dun1 FHA-Dif1 interaction strength with the K136A mutation.

Neither mutants of the lateral surface interaction patch nor the pThr-binding site were able to individually result in complete disruption of the Dun1-Sml1 interaction, but they did individually reduce the strength of the interaction. A likely scenario, and one that needs to be tested, is whether a combined mutant of both regions would completely disrupt the interaction between Dun1 and Sml1. Another particularly useful examination would be to conduct a pull-down assay using purified Dun1, Dif1, and Sml1 expressed from bacterial plasmids in *Escherichia coli* (*E. coli*) to determine whether the Dun1-Dif1 and Dun1-Sml1 interactions observed using yeast two-hybrid assays are direct physical interactions or indirect. In the event that the interactions are direct, collaborating with a structural biology lab to solve the co-crystal structure between the Dun1 FHA domain and full-length Dif1 and maybe full-length Dun1

and Sml1 would prove invaluable to a comprehensive analysis of the Dun1 lateral surface interaction patch by depicting the exact residues involved in the interactions. Additionally, generating Dun1 FHA domain mutations within the budding yeast genome instead of utilizing expression from an external plasmid could be used to bypass the apparent inactivity of Bleomycin, Phleomycin, and Camptothecin on selective SC media. Spot plate assays evaluating genotoxic sensitivity to other compounds besides HU and MMS could reveal a more distinct phenotypic effect of Dun1 FHA mutants that have compromised protein-protein interactions that are involved in the dNTP regulation pathway.

4.3 Impact and Relevance of FHA Domain Research

The canonical pThr-binding site is a prominent feature of FHA domains. Until recently, the scope of research done on FHA domain-based protein-protein interactions did not extend beyond analyzing the contribution of the pThr-binding site as the means of FHA domain ligand recognition (reviewed in Mahajan et al., 2008). The discovery of the non-canonical FHA domain lateral surface interaction patch in the FHA1 domain of budding yeast Rad53 and the characterization of its contribution to the interaction between the FHA1 domain of Rad53 and the H-BRCT domain of Dbf4 paved the way for researchers to broaden their vantage point when studying protein-protein interactions involving FHA domains (Matthews et al., 2014). The research presented in this thesis confirming both the existence and contribution of a conserved non-canonical FHA domain lateral surface interaction patch in another FHA domain-containing protein, proves that the existence of a lateral surface interaction patch within an FHA domain is not a unique feature of Rad53 FHA1. It demonstrates the importance of studying this non-canonical FHA domain lateral surface interaction patch as a potential interaction interface in other FHA domain-containing proteins. Since FHA domains are common amongst cell cycle regulation and checkpoint proteins, a more comprehensive examination of FHA domains and the protein-protein interactions that they mediate via the study of the occurrence and contribution of non-canonical FHA domain lateral surface interaction patches in FHA domain-containing proteins could unveil the true

complexities of cell cycle regulation and checkpoints. Such revelations would advance our understanding of cell cycle progression and regulation errors, key contributors to cancer and cancer-related diseases. Such revelations will advance our techniques for preventative and post-diagnostic care for such diseases by giving us the means to design targeted therapeutic tactics to attack the specific problems of disease thereby avoiding the systemic damage that remains a prominent side-effect of treatments such as chemotherapy and radiation.

Bibliography

Allen, J. B., Zhou, Z., Siede, W., Friedberg, E. C., & Elledge, S. J. (1994). The SAD1/RAD53 protein kinase controls multiple checkpoints and DNA damage-induced transcription in yeast. *Genes & Development, 8*(20), 2401-2415.

Ausubel, F. M., Brent, R., Kinston, R., Moore, D., Seidman, J. J., Smith, J., Struhl, K. eds. (1994). *Current Protocols in Molecular Biology*. (Wiley, New York).

Andreson, B. L., Gupta, A., Georgieva, B. P., & Rothstein, R. (2010). The ribonucleotide reductase inhibitor, Sml1, is sequentially phosphorylated, ubiquitylated and degraded in response to DNA damage.*38*(19), 6490-6501.

Balasubramanian, M. K., Bi, E., & Glotzer, M. (2004). *Comparative analysis of cytokinesis in budding yeast, fission yeast and animal cells*.

Barnum, K. J., & O'Connell, M. J. (2014). Cell cycle regulation by checkpoints. *Methods in Molecular Biology (Clifton, N.J.), 1170*, 29-40.

Bashkirov, V. I., Bashkirova, E. V., Haghnazari, E., & Heyer, W. D. (2003). Direct kinase-to-kinase signaling mediated by the FHA phosphoprotein recognition domain of the Dun1 DNA damage checkpoint kinase. *Molecular and Cellular Biology, 23*(4), 1441-1452.

Chabes, A., Domkin, V., & Thelander, L. (1999). Yeast Sml1, a protein inhibitor of ribonucleotide reductase. *The Journal of Biological Chemistry, 274*(51), 36679-36683.

Chen, S., Smolka, M. B., & Zhou, H. (2007). Mechanism of Dun1 activation by Rad53 phosphorylation in saccharomyces cerevisiae. *The Journal of Biological Chemistry, 282*(2), 986-995.

Clarke, L., & Carbon, J. (1980). Isolation of a yeast centromere and construction of functional small circular chromosomes. *Nature, 287*(5782), 504-509.

Dobson, M. J., Pickett, A. J., Velmurugan, S., Pinder, J. B., Barrett, L. A., Jayaram, M., & Chew, J. S. K. (2005). The 2µm plasmid causes cell death in saccharomyces cerevisiae with a mutation in Ulp1 protease. *Molecular and Cellular Biology, 25*(10), 4299-4310.

Dohrmann, P. R., & Sclafani, R. A. (2006). Novel role for checkpoint Rad53 protein kinase in the initiation of chromosomal DNA replication in saccharomyces cerevisiae. *Genetics, 174*(1), 87-99.

Duina, A. A., Miller, M. E., & Keeney, J. B. (2014). Budding yeast for budding geneticists: A primer on the saccharomyces cerevisiae model system. *Genetics, 197*(1), 33-48.

Duncker, B. P., Shimada, K., Tsai-Pflugfelder, M., Pasero, P., & Gasser, S. M. (2002). An N-terminal domain of Dbf4p mediates interaction with both origin recognition complex (ORC) and Rad53p and can deregulate late origin firing. *Proceedings of the National Academy of Sciences, 99*(25), 16087-16092.

Durocher, D., Jackson, S. P. (2002). The FHA domain. *FEBS Letters*. 513: 58-66

Gershon, H., & Gershon, D. (2000). The budding yeast, saccharomyces cerevisiae, as a model for aging research: A critical review. *Mechanisms of Ageing and Development, 120*(1-3), 1-22.

Goffeau, A., Barrell, B. G., Bussey, H., Davis, R. W., Dujon, B., Feldmann, H., Galibert, G., Hoheisel, J. D., Johnston, M., Louis, E. J., Mewes, H. W., Murakami, Y., Philippsen, P., Tettelin, H., & Oliver, S. G. (1996). Life with 6000 genes. *Science (New York, N.Y.), 274*(5287), 546, 563-7.

Guitor, A. Characterizing non-canonical forkhead-associated domain-binding interfaces in *Saccharomyces cerevisiae*. [Senior Honours Thesis]. University of Waterloo; 2016. 55 p.

Gyuris, J., Golemis, E., Chertkov, H., & Brent, R. (1993). Cdi1, a human G1 and S phase protein phosphatase that associates with Cdk2. *Cell, 75*(4), 791-803.

Harashima, H., Dissmeyer, N., & Schnittger, A. (2013). Cell cycle control across the eukaryotic kingdom. *Trends in Cell Biology, 23*(7), 345-356.

Herskowitz, I. (1988). Life cycle of the budding yeast saccharomyces cerevisiae. *Microbiological Reviews, 52*(4), 536-553.

Hofmann, K., Bucher, P. (1995). The FHA domain: a putative nuclear signalling domain found in protein kinases and transcription factors. *Trends Biochem Sci*. 20(9): 347-349.

Huang, M., & Elledge, S. J. (1997). Identification of RNR4, encoding a second essential small subunit of ribonucleotide reductase in saccharomyces cerevisiae. *Molecular and Cellular Biology, 17*(10), 6105-6113.

Huang, M., Zhou, Z., & Elledge, S. J. (1998). The DNA replication and damage checkpoint pathways induce transcription by inhibition of the Crt1 repressor. *Cell, 94*(5), 595-605.

Huh, W. K., Falvo, J. V., Gerke, L. C., Carroll, A. S., Howson, R. W., Weissman, J. S., & O'Shea, E. K. (2003). Global analysis of protein localization in budding yeast. *Nature, 425*(6959), 686-691.

Ishii, J., Izawa, K., Matsumura, S., Wakamura, K., Tanino, T., Tanaka, T., Ogino, C., Fukuda, H., & Kondo, A. (2009). A simple and immediate method for simultaneously evaluating expression level and plasmid maintenance in yeast. *Journal of Biochemistry, 145*(6), 701-708.

Koivomagi, M., Valk, E., Venta, R., Iofik, A., Lepiku, M., Morgan, D., & Loog, M. (2011). Dynamics of Cdk1 substrate specificity during the cell cycle. *Molecular Cell, 42*(5-4), 610-623.

Lee, H., Yuan, C., Hammet, A., Mahajan, A., Chen, E. S., Wu, M. R., Su, M. I., Heierhorst, J., & Tsai, M. D. (2008). Diphosphothreonine-specific interaction between an SQ/TQ cluster and an FHA domain in the Rad53-Dun1 kinase cascade. *Molecular Cell, 30*(6), 767-778.

Lee, S. J., Schwartz, M. F., Duong, J. K., & Stern, D. F. (2003). Rad53 phosphorylation site clusters are important for Rad53 regulation and signaling. *Molecular and Cellular Biology, 23*(17), 6300-6314.

Lee, Y. D., & Elledge, S. J. (2006). Control of ribonucleotide reductase localization through an anchoring mechanism involving Wtm1. *Genes & Development, 20*(3), 334-344.

Lee, Y. D., Wang, J., Stubbe, J. A., & Elledge, S. J. (2008). Dif1 is a DNA damage regulated facilitator of nuclear import for ribonucleotide reductase. *Molecular Cell, 32*(1), 70-80.

Lehne, B., Schlitt, T. (2009). Protein-protein interaction databases: Keeping up with growing interactomes. *Human Genomics*. 3(3): 291-297.

Longhese, M. P., Paciotti, V., Fraschini, R., Zaccarini, R., Plevani, P., & Lucchini, G. (1997). The novel DNA damage checkpoint protein ddc1p is phosphorylated periodically during the cell cycle and in response to DNA damage in budding yeast. *The EMBO Journal, 16*(17), 5216-5226.

Mahajan, A., Yuan, C., Lee, H., Chen, E. S. W., Wu, P., Tsai, M. (2008). Structure and Function of the Phosphothreonine-Specific FHA Domain. *Science Signaling*. 1(51): 1-18.

Matthews, L. A., Jones, D. R., Prasad, A. A., Duncker, B. P., Guarne, A. (2012). *Saccharomyces cerevisiae* Dbf4 Has Unique Fold Necessary for Interaction with Rad53 Kinase. *J. Biol. Chem*. 287(4): 2378-2387.

Matthews, L. A., Selvaratnam, R., Jones, D. R., Akimoto, M., McConkey, B. J., Melacini, G., Duncker, B. P., Guarne, A. (2014). A Novel Non-canonical Forkhead-associated (FHA) Domain-binding Interface Mediates the Interaction between Rad53 and Dbf4 Proteins. *J. Biol. Chem.* 289(5): 2589-2599.

Mohammad, D. H., Yaffe, M. B. (2009). 14-3-3 Proteins, FHA Domains and BRCT Domains in the DNA Damage Response. *DNA Repair (Amst)*. 8(9): 1009-1017.

Morgan, D. O. (1997). Cyclin-dependent kinases: Engines, clocks, and microprocessors. *Annual Review of Cell and Developmental Biology, 13*, 261-291.

Mortimer, R. K. (2000). Evolution and variation of the yeast (saccharomyces) genome. *Genome Research, 10*(4), 403-409.

Mortimer, R. K., & Johnston, J. R. (1986). Genealogy of principal strains of the yeast genetic stock center. *Genetics, 113*(1), 35-43.

Nasmyth, K. (1996). At the heart of the budding yeast cell cycle. *Trends in Genetics, 12*(10), 405-412.

Paulovich, A. G., & Hartwell, L. H. (1995). A checkpoint regulates the rate of progression through S phase in S. cerevisiae in response to DNA damage. *Cell, 82*(5), 841-847.

Pemberton, L. F., & Blobel, G. (1997). Characterization of the wtm proteins, a novel family of saccharomyces cerevisiae transcriptional modulators with roles in meiotic regulation and silencing. *Molecular and Cellular Biology, 17*(8), 4830-4841.

Rhind, N., & Russell, P. (1998). Mitotic DNA damage and replication checkpoints in yeast. *Current Opinion in Cell Biology, 10*(6), 749-758.

Robertson, A. (2015). Characterization of novel FHA domain ligand binding motifs. [Master of Science Thesis]. University of Waterloo. 122 p.

Sanvisens, N., Romero, A. M., An, X., Zhang, C., de Llanos, R., Martinez-Pastor, M. T., Bano, M. C., Huang, M., & Puig, S. (2014). Yeast Dun1 kinase regulates ribonucleotide reductase inhibitor Sml1 in response to iron deficiency. *Molecular and Cellular Biology, 34*(17), 3259-3271.

Sanvisens, N., Romero, A. M., Zhang, C., Wu, X., An, X., Huang, M., Puig, S. (2016). Yeast Dun1 Kinase Regulates Ribonucleotide Reductase Small Subunit Localization in Response to Iron Deficiency. *J. Biol. Chem.* 291(18): 9807-9817.

Shirahige, K., Hori, Y., Shiraishi, K., Yamashita, M., Takahashi, K., Obuse, C., Tsurimoto, T., Yoshikawa, H. (1998). Regulation of DNA-replication origins during cell cycle progression. *Nature*. 395: 618-621.

Siede, W., Friedberg, A. S., Dianova, I., & Friedberg, E. C. (1994). Characterization of G1 checkpoint control in the yeast saccharomyces cerevisiae following exposure to DNA-damaging agents. *Genetics, 138*(2), 271-281.

Siede, W., Friedberg, A. S., & Friedberg, E. C. (1993). RAD9-dependent G1 arrest defines a second checkpoint for damaged DNA in the cell cycle of saccharomyces cerevisiae. *Proceedings of the National Academy of Sciences, 90*(17), 7985-7989.

Stearns, T., Ma, H., & Botstein, D. (1990). Manipulating yeast genome using plasmid vectors. *Methods in Enzymology, 185*, 280-297.

Tam, A. T., Pike, B. L., & Heierhorst, J. (2008). Location-specific functions of the two forkhead-associated domains in Rad53 checkpoint kinase signaling. *Biochemistry, 47*(12), 3912-3916.

Tsaponina, O., Barsoum, E., Astrom, S. U., & Chabes, A. (2011). Ixr1 is required for the expression of the ribonucleotide reductase Rnr1 and maintenance of dNTP pools. *PLoS Genetics, 7*(5), e1002061.

Weinert, T. A., & Hartwell, L. H. (1988). The RAD9 gene controls the cell cycle response to DNA damage in saccharomyces cerevisiae. *Science (New York, N.Y.), 241*(4863), 317-322.

Weinert, T. A., Kiser, G. L., & Hartwell, L. H. (1994). Mitotic checkpoint genes in budding yeast and the dependence of mitosis on DNA replication and repair. *Genes & Development, 8*(6), 652-665.

Yoshitani, A., Ling, F., Yoshida, M. (2008). The Yeast Checkpoint Kinase Dun1 Downregulates *DIN7* in the Absence of DNA Damage. *Biosci. Biotechnol. Biochem.* 72(6): 1630-1634.

Zhang, Z., Yang, K., Chen, C. C., Feser, J., & Huang, M. (2007). Role of the C terminus of the ribonucleotide reductase large subunit in enzyme regeneration and its inhibition by Sml1. *Proceedings of the National Academy of Sciences of the United States of America, 104*(7), 2217-2222.

Zhao, X., Georgieva, B., Chabes, A., Domkin, V., Ippel, J. H., Schleucher, J., Wijmenga, S., Thelander, L., & Rothstein, R. (2000). Mutational and structural analyses of the ribonucleotide reductase inhibitor Sml1 define its Rnr1 interaction domain whose inactivation allows suppression of mec1 and rad53 lethality. *Molecular and Cellular Biology, 20*(23), 9076-9083.

Zhao, X., Muller, E. G., & Rothstein, R. (1998). A suppressor of two essential checkpoint genes identifies a novel protein that negatively affects dNTP pools. *Molecular Cell, 2*(3), 329-340.

Zhao, X., & Rothstein, R. (2002). The Dun1 checkpoint kinase phosphorylates and regulates the ribonucleotide reductase inhibitor Sml1. *Proceedings of the National Academy of Sciences of the United States of America, 99*(6), 3746-3751.

Zhou, Z., & Elledge, S. J. (1993). DUN1 encodes a protein kinase that controls the DNA damage response in yeast. *Cell, 75*(6), 1119-1127.